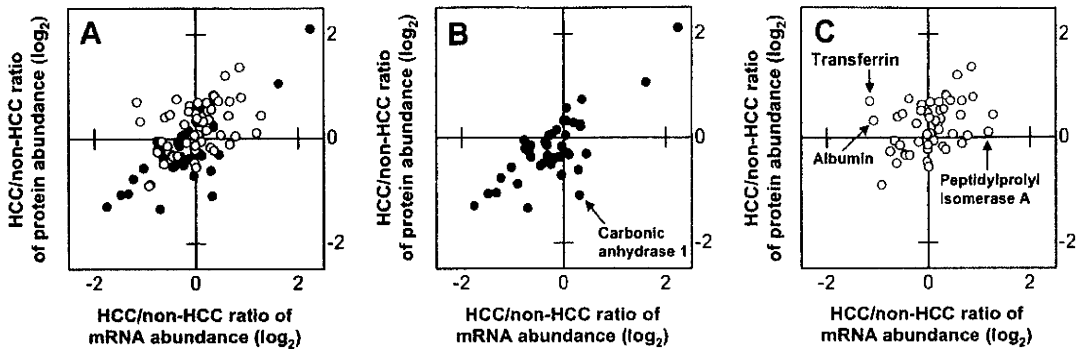

Fig. 2. Comparative analysis of protein and mRNA expression profiles between HCC and non-HCC. (A) The HCC/non-HCC ratios of averaged protein expression levels for 93 proteins were plotted against those of mRNA. Proteins related to metabolic pathways were indicated in closed circles and were shown again in (B). Proteins related to the other biochemical pathways were indicated in open circles and shown in (C). Proteins listed in Table 3 were indicated in (B) and (C). All graphs were depicted in $\log_2$ scale.

Table 3
Proteins whose expression changes between HCC and non-HCC show poor correlation to mRNA expression changes

Spot ID	Protein name	Refseq ID	Theoretical		Spot[a] Av. Ratio	Spot *p* value	Protein ratio	Micro array Av. ratio	Micro array *p* value
			*p*I	MW (kDa)					
564	Transferrin	NP_001054	6.8	79.3	2.23	0.035	1.61	0.45	3.3E−06
565					1.87	0.079			
566					2.28	0.13			
605					0.73	0.098			
1489	Albumin	NP_000468	5.9	71.3	—	0.63	1.25	0.47	2.3E−03
1941	Carbonic anhydrase 1	NP_001729	6.6	28.9	—	3.5E−03	0.47	1.25	0.39
2290	Peptidylprolyl isomerase A	NP_066953	7.7	18.1	—	5.0E−01	1.07	2.29	1.1E−01

[a] Since transferrin was detected in multiple spots, averaged ratio and spot *p* value of each spot is shown.

Table 4
Multi-spotted proteins showing spot-to-spot differences in expression level between non-HCC and HCC

Spot ID	Spot Av. ratio	Spot *p* value	Protein name	Refseq ID	Theoretical		Protein[a] ratio
					*p*I	MW (kDa)	
436	1.92	5.3E−04	Tumor rejection antigen (gp96)	NP_003290	4.8	92.7	1.2
537	0.79	0.16					
564	2.23	0.035	Transferrin	NP_001054	6.8	79.3	1.61
565	1.87	0.079					
566	2.28	0.13					
605	0.73	0.098					
1257	1.02	0.92	Fumarate hydratase	NP_000134	8.8	54.8	0.8
1261	0.6	1.3E−03					

[a] HCC/non-HCC protein ratios were calculated using integrated spot abundances.

gene expression was done with BRB-ArrayTools (http://linus.nci.nih.gov/BRB-ArrayTools.htm). The filtered data were log-transferred, normalized, centered, and applied to the average linkage clustering with centered correlation. BRB-ArrayTools contains a class comparison tool based on univariate *F* tests to find genes differentially expressed between predefined clinical groups. The permutation distribution of the *F* statistic, based on 2000 random permutations, was also used to confirm statistical significance. A *p* value of less than 0.05 for differences in HCC/non-HCC gene expression ratio was considered significant.

The average HCC/non-HCC expression ratios of the 93 proteins were plotted against the mRNA ratios in Fig. 2, where a positive value indicates increased expression in HCC and a negative ratio indicates reduced expression. The overall expression ratio of HCC/non-HCC indicated noticeable correlation between protein and mRNA

(Fig. 2A), and the Pearson's correlation coefficient for this data set (93 proteins/genes) was 0.73. Next, we divided 93 proteins into those related to metabolism and others biological processes. The HCC/non-HCC ratios of protein expression for metabolism-related proteins showed substantial correlation with those of mRNA (Fig. 2B, $r = 0.9$), whereas those of other proteins were poorly correlated (Fig. 2C, $r = 0.36$). Extreme care must be taken in a direct comparison of proteomic data with transcriptome because of multiple layers of discrepancies caused by the distinct sensitivities of cDNA array hybridization and 2-DE, the inability of a cDNA array to distinguish mRNA isoforms and post-translational modifications of proteins. Nevertheless, our results suggest that the expression of considerable portion of proteins with metabolic function listed here is regulated at transcriptional level. On the other hand, post-transcriptional and/or post-translational processes seem to be involved in the regulation of expression level for proteins with other cellular functions as a whole. Four proteins (albumin, transferrin, peptidylproryl isomerase A, and carbonic anhydrase 1) showed apparent poor correlation in protein and mRNA expression profiles (Table 3 and Fig. 2). Transcriptional control might have little effect on the expression changes of these proteins between HCC and non-HCC.

A number of proteins were expressed as multiple spots on 2-DE gels and most multi-spotted proteins showed little spot-to-spot variations in the averaged HCC/non-HCC ratio. Although we do not know how these multiple spots were generated, many of them might be due to the conformational equilibrium of proteins under electrophoresis rather than to any post-translational modifications [28]. On the other hand, the HCC/non-HCC expression ratios of several multi-spotted proteins varied from spot to spot, and three proteins (transferrin, fumarate hydratase, and tumor rejection antigen gp96) were categorized as these multi-spotted proteins (Table 4).

For example, gp96 was detected in two spots (spot #436 and 537) with distinct molecular mass and p*I* and they showed different HCC/non-HCC expression ratio (Fig. 3A and B and Table 4). The expression of these two isoforms was observed to change in the opposite direction between non-HCC and HCC: #436 was up-regulated in HCC (HCC/non-HCC ratio: 1.96) while #537 was down-regulated (HCC/non-HCC ratio: 0.79) (Table 4 and Fig. 3C and D). Gp96 is a glycoprotein present in endoplasmic reticulum and is supposed to function as a molec-

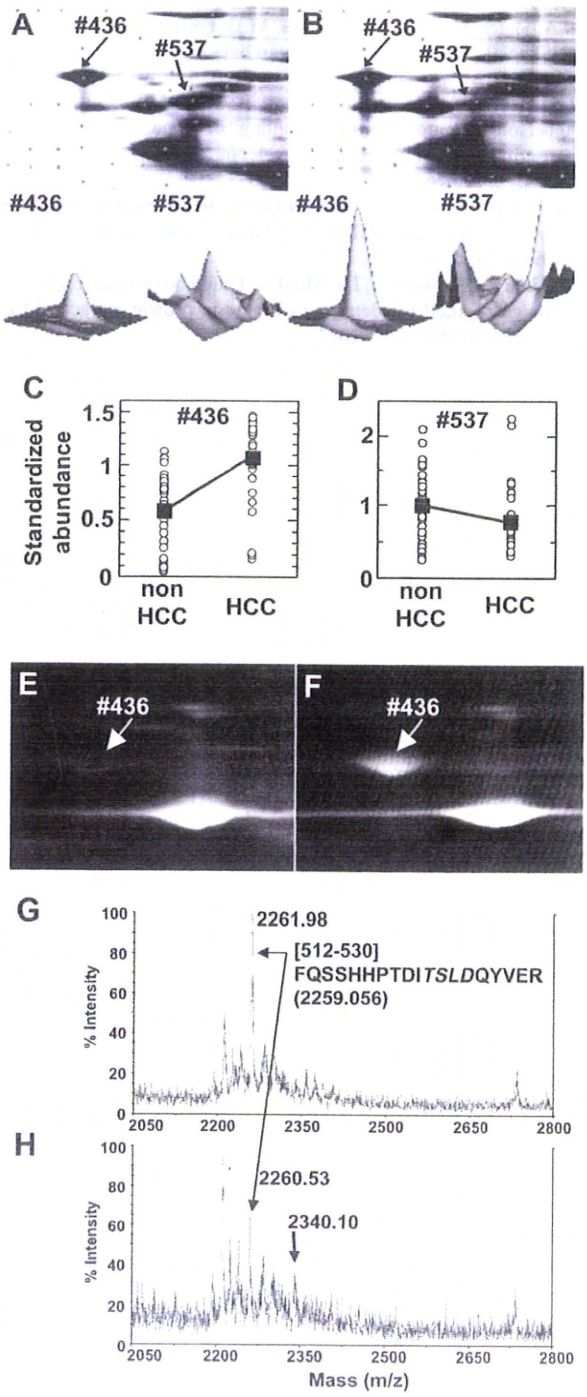

Fig. 3. Comparison of expression profiles of two gp96 spots between HCC and non-HCC. The expression profile and phosphorylation of tumor rejection antigen gp96 in HCC and non-HCC was investigated. Magnified gel images and 3D views of two gp96 spots in non-HCC (A) and HCC (B) were shown. Differences in expression level of two gp96 spots, #436 (C) and #537 (D), between non-HCC and HCC were shown. The open circle indicates the standardized abundance of the individual spot in each sample. The closed square represents the averaged abundance of each gp96 spot. Magnified gel images of non-HCC (E) and HCC (F) stained with ProQ. The #436 spot was positively stained with ProQ, while unambiguous staining of the #537 spot was not observed. Tryptic peptides prepared from the spot #436 were analyzed by MALDI–TOF mass-spectrometry in the positive ion mode (G) and the negative ion mode (H). A peak of 2261.98 detected in positive ion mode corresponds to the amino acid sequence from 512 to 530. In addition to the original peak (*m/z*: 2260.53), a peak mass shifted by +80 Da was detected in the negative ion mode. A predicted phosphorylation consensus motif for protein kinase CK2 is indicated in italics (G).

ular chaperone and intracellular Ca^{2+} regulator [29,30]. Several previous reports have shown that gp96 is glycosylated and phosphorylated, and exists as heterogeneous molecular entities with various molecular weights [31]. In order to know whether gp96 spots were phosphorylated or not, we stained the 2-DE gels with ProQ Diamond which is a dye specific to proteins phosphorylated on serine, threonine or tyrosine residues [32], and has been used successfully to visualize phosphoproteins [33]. We found that the spot #436 was positively stained with ProQ (Fig. 3E and F). We further tried to detect possible phosphorylated peptides in the tryptic digests prepared from #436 by MALDI–TOF–MS according to Nabetani et al. [21]. Searching for those peaks that had relatively stronger intensities in negative ion mode than in positive ion mode, we found two peaks as candidates for acidically modified peptides. They were assigned to the peptides SILFVPTSAPR (amino acid sequence: 385–395, data not shown) and FQSSHHPTDITSLDQYVER (aa512–530). Fig. 3G and H show the unmodified peak and the acidically modified peak (mass shifted by +80 Da in negative ion mode) of the latter peptide, respectively. This peptide contained a predicted phosphorylation consensus motif, [Ser or Thr]-X-X-[Asp or Glu], for protein kinase CK2 (Fig. 3G) which was suggested to phosphorylate gp96 [34]. These results together with ProQ staining indicated that at least one gp96 isoform was phosphorylated and was up-regulated in HCC. Over-expression of gp96 in HCC has been reported previously [35], though the reports that showed over-expression of its phosphorylated form are rare. Further investigation into biological meaning of gp96 phosphorylation may provide us important information about HCC development.

Acknowledgments

We thank the late Dr. A. Tsugita for helpful discussion through this work and N. Tetsura for technical assistance.

Appendix A. Supplementary data

Supplementary data associated with this article can be found, in the online version, at doi:10.1016/j.bbrc.2007.11.101.

References

[1] T.K. Seow, R.C.M.Y. Liang, C.K. Leow, M.C.M. Chung, Hepatocellular carcinoma: from bedside to proteomics, Proteomics 1 (2001) 1249–1263.

[2] L.J. Lopez, J.A. Marrero, Hepatocellular carcinoma, Curr. Opin. Gastroenterol. 3 (2004) 248–253.

[3] H.F. Kawai, S. Kaneko, M. Honda, Y. Shirota, K. Kobayashi, Alpha-fetoprotein-producing hepatoma cell lines share common expression profiles of genes in various categories demonstrated by cDNA microarray analysis, Hepatology 3 (2001) 676–691.

[4] N. Iizuka, M. Oka, H. Yamada-Okabe, N. Mori, T. Tamesa, T. Okada, N. Takemoto, K. Hashimoto, et al., Differential gene expression in distinct virologic types of hepatocellular carcinoma: association with liver cirrhosis, Oncogene 22 (2003) 3007–3014.

[5] T. Yamashita, S. Kaneko, S. Hashimoto, T. Sato, S. Nagai, N. Toyoda, T. Suzuki, K. Kobayashi, et al., Serial analysis of gene expression in chronic hepatitis C and hepatocellular carcinoma, Biochem. Biophys. Res. Commun. 282 (2001) 647–654.

[6] K. Kawaguchi, M. Honda, T. Yamashita, Y. Shirota, S. Kaneko, Differential gene alteration among hepatoma cell lines demonstrated by cDNA microarray-based comparative genomic hybridization, Biochem. Biophys. Res. Commun. 329 (2005) 370–380.

[7] Y. Midorikawa, M. Makuuchi, W. Tang, H. Aburatani, Microarray-based analysis for hepatocellular carcinoma: from gene expression profiling to new challenges, World J. Gastroenterol. 13 (2007) 1487–1492.

[8] N.A. Shackel, D. Seth, P.S. Haber, M.D. Gorrell, G.W. McCaughan, The hepatic transcriptome in human liver disease, Comp. Hepatol. 5 (6) (2006).

[9] T.J. Griffin, S.P. Gygi, T. Ideker, B. Rist, J. Eng, L. Hood, R. Aebersold, Complementary profiling of gene expression at the transcriptome and proteome levels in *Saccharomyces cerevisiae*, Mol. Cell. Proteomics 4 (2002) 323–333.

[10] S.P. Gygi, Y. Rochon, B.R. Franza, R. Aebersold, Correlation between protein and mRNA abundance in yeast, Mol. Cell. Biol. 19 (1999) 1720–1730.

[11] M. Unlu, M.E. Morgan, J.S. Minden, Difference gel electrophoresis: a single gel method for detecting changes in protein extracts, Electrophoresis 11 (1997) 2071–2077.

[12] I.N. Lee, C.H. Chen, J.C. Sheu, H.S. Lee, G.T. Huang, C.Y. Yu, F.J. Lu, L.P. Chow, Identification of human hepatocellular carcinoma-related biomarkers by two-dimensional difference gel electrophoresis and mass spectrometry, J. Proteome Res. 6 (2005) 2062–2069.

[13] C.R. Liang, C.K. Leow, J.C. Neo, G.S. Tan, S.L. Lo, J.W. Lim, T.K. Seow, P.B. Lai, et al., Proteome analysis of human hepatocellular carcinoma tissues by two-dimensional difference gel electrophoresis and mass spectrometry, Proteomics 5 (2005) 2258–2271.

[14] V.J. Desmet, M. Gerber, J.H. Hoofnagle, M. Manns, P.J. Scheuer, Classification of chronic hepatitis: diagnosis, grading and staging, Hepatology 19 (1994) 1513–1520.

[15] K.G. Ishak, P.P. Anthony, L.H. Sobin, Histological typing of tumours of the liver, 2nd ed.WHO International Histological Classification of Tumors, Springer-Verlag, New York, 1994.

[16] M. Honda, S. Kaneko, H. Kawai, Y. Shirota, K. Kobayashi, Differential gene expression between chronic hepatitis B and C hepatic lesion, Gastroenterology 120 (2001) 955–966.

[17] H.F. Kawai, S. Kaneko, M. Honda, Y. Shirota, K. Kobayashi, Alpha-fetoprotein-producing hepatoma cell lines share common expression profiles of genes in various categories demonstrated by cDNA microarray analysis, Hepatology 33 (2001) 676–691.

[18] M. Honda, H. Kawai, Y. Shirota, T. Yamashita, T. Takamura, S. Kaneko, cDNA microarray analysis of autoimmune hepatitis, primary biliary cirrhosis and consecutive disease manifestation, J. Autoimmun. 25 (2005) 133–140.

[19] M. Honda, T. Yamashita, T. Ueda, H. Takatori, R. Nishino, S. Kaneko, Different signaling pathways in the livers of patients with chronic hepatitis B or chronic hepatitis C, Hepatology 44 (2006) 1122–1138.

[20] Y. Tabuse, T. Nabetani, A. Tsugita, Proteomic analysis of protein expression profiles during *Caenorhabditis elegans* development using 2D-difference gel electrophores, Proteomics 5 (2005) 2876–2891.

[21] T. Nabetani, K. Miyazaki, Y. Tabuse, A. Tsugita, Analysis of acidic peptides with a matrix-assisted laser desorption/ionization mass spectrometry using positive and negative ion modes with additive monoammonium phosphate, Proteomics 6 (2006) 4456–4465.

[22] Y. Kuramitsu, T. Harada, M. Takashima, Y. Yokoyama, I. Hidaka, N. Iizuka, T. Toda, M. Fujimoto, et al., Increased expression and phosphorylation of liver glutamine synthetase in well-differentiated

hepatocellular carcinoma tissues from patients infected with hepatitis C virus, Electrophoresis 27 (2006) 1651–1658.
[23] L. Hu, S.H. Lau, C.H. Tzang, J.M. Wen, W. Wang, D. Xie, M. Huang, Y. Wang, et al., Association of Vimentin overexpression and hepatocellular carcinoma metastasis, Oncogene 23 (2004) 298–302.
[24] Z. Dai, Y.K. Liu, J.F. Cui, H.L. Shen, J. Chen, R.X. Sun, Y. Zhang, X.W. Zhou, Identification and analysis of altered alpha1,6-fucosylated glycoproteins associated with hepatocellular carcinoma metastasis, Proteomics 6 (2006) 5857–5867.
[25] E. Zeindl-Eberhart, S. Haraida, S. Liebmann, P.R. Jungblut, S. Lamer, D. Mayer, G. Jäger, S. Chung, H.M. Rabes, Detection and identification of tumor-associated protein variants in human hepatocellular carcinomas, Hepatology 39 (2004) 540–549.
[26] W.H. Kuo, W.L. Chiang, S.F. Yang, K.T. Yeh, C.M. Yeh, Y.S. Hsieh, S.C. Chu, The differential expression of cytosolic carbonic anhydrase in human hepatocellular carcinoma, Life Sci. 73 (2003) 2211–2223.
[27] P.N. Cheng, T.L. Lam, W.M. Lam, S.M. Tsui, A.W. Cheng, W.H. Lo, Y.C. Leung, Pegylated recombinant human arginase (rhArg-peg5,000mw) inhibits the in vitro and in vivo proliferation of human hepatocellular carcinoma through arginine depletion, Cancer Res. 67 (2007) 309–317.
[28] F.S. Berven, O.A. Karisen, J.C. Murrell, H.B. Jensen, Multiple polypeptide forms observed in two-dimensional gels of Methylococcus capsulatus (Bath) polypeptides are generated during the separation procedure, Electrophoresis 24 (2003) 757–761.
[29] J. Melnick, S. Aviel, Y. Argon, The endoplasmic reticulum stress protein GRP94, in addition to BiP, associates with unassembled immunoglobulin chains, J. Biol. Chem. 267 (1992) 21303–21306.
[30] H. Liu, E. Miller, B. van de Water, J.L. Stevens, Endoplasmic reticulum stress proteins block oxidant-induced Ca^{2+} increases and cell death, J. Biol. Chem. 273 (1998) 12858–12862.
[31] A.M. Feldweg, P.K. Srivastava, Molecular heterogeneity of tumor rejection antigen/heat shock protein GP96, Int. J. Cancer 63 (1995) 310–314.
[32] T.H. Steinberg, B.J. Agnew, K.R. Gee, W.-Y. Leung, T. Goodman, B. Schulenberg, J. Hendrickson, J.M. Beechem, R.P. Haugland, W.F. Patton, Global quantitative phosphoprotein analysis using multiplexed proteomics technology, Proteomics 3 (2003) 1128–1144.
[33] B.R. Chitteti, Z. Peng, Proteome and phosphoproteome dynamic change during cell dedifferentiation in Arabidopsis, Proteomics 7 (2007) 1473–1500.
[34] S.E. Cala, GRP94 hyperglycosylation and phosphorylation in Sf21 cells, Biochim. Biophys. Acta 1496 (2000) 296–310.
[35] D.F. Yao, X.H. Wu, X.Q. Su, M. Yao, W. Wu, L.W. Qiu, L. Zou, X.Y. Meng, Abnormal expression of HSP gp96 associated with HBV replication in human hepatocellular carcinoma, Hepatobiliary Pancreat. Dis. Int. 5 (2006) 381–386.

JOURNAL OF VIROLOGY, Sept. 2010, p. 9118–9127
0022-538X/10/$12.00 doi:10.1128/JVI.00402-10

Vol. 84, No. 18

A Disulfide-Bonded Dimer of the Core Protein of Hepatitis C Virus Is Important for Virus-Like Particle Production▽†

Yukihiro Kushima,[1,2] Takaji Wakita,[3] and Makoto Hijikata[1,2]*

Department of Viral Oncology, Institute for Virus Research, Kyoto University, Kyoto 606-8507, Japan[1]; Graduate School of Biostudies, Kyoto University, Kyoto 606-8507, Japan[2]; and Department of Virology II, National Institute of Infectious Diseases, Tokyo 162-8640, Japan[3]

Received 24 February 2010/Accepted 20 June 2010

Hepatitis C virus (HCV) core protein forms the nucleocapsid of the HCV particle. Although many functions of core protein have been reported, how the HCV particle is assembled is not well understood. Here we show that the nucleocapsid-like particle of HCV is composed of a disulfide-bonded core protein complex (dbc-complex). We also found that the disulfide-bonded dimer of the core protein (dbd-core) is formed at the endoplasmic reticulum (ER), where the core protein is initially produced and processed. Mutational analysis revealed that the cysteine residue at amino acid position 128 (Cys128) of the core protein, a highly conserved residue among almost all reported isolates, is responsible for dbd-core formation and virus-like particle production but has no effect on the replication of the HCV RNA genome or the several known functions of the core protein, including RNA binding ability and localization to the lipid droplet. The Cys128 mutant core protein showed a dominant negative effect in terms of HCV-like particle production. These results suggest that this disulfide bond is critical for the HCV virion. We also obtained the results that the dbc-complex in the nucleocapsid-like structure was sensitive to proteinase K but not trypsin digestion, suggesting that the capsid is built up of a tightly packed structure of the core protein, with its amino (N)-terminal arginine-rich region being concealed inside.

Hepatitis C virus (HCV) infection is a major cause of chronic hepatitis, liver cirrhosis, and hepatocellular carcinoma, affecting approximately 200 million people worldwide (13, 29, 44). Current treatment strategies, including interferon coupled with ribavirin, are not effective for all patients infected with HCV. An error-prone replication strategy allows HCV to undergo rapid mutational evolution in response to immune pressure and thus evade adaptive immune responses (10). New approaches to HCV therapy include the development of specifically targeted antiviral therapies for hepatitis C (STAT-Cs) which target such HCV proteins as the nonstructural 3/4A (NS3/4A), serine protease, and RNA-dependent RNA polymerase NS5B proteins (3). Despite the potent antiviral activities of some of these approaches, many resistant HCV strains have been reported after treatment with existing STAT-Cs (23, 48, 51). Therefore, identification of new targets that are common to all HCV strains and that are associated with low mutation rates is an area of active research.

HCV has a 9.6-kb, plus-strand RNA genome composed of a 5′ untranslated region (UTR), an open reading frame that encodes a single polyprotein of about 3,000 amino acids, and a 3′ UTR. The polyprotein is processed by host and viral proteases to produce three structural proteins (the core, envelope 1 [E1], and E2 proteins) and seven nonstructural proteins (the p7, NS2, NS3, NS4A, NS4B, NS5A, and NS5B proteins) (14, 16, 17, 22, 49). The HCV core protein is produced cotranslationally via carboxyl (C)-terminal cleavage to generate an immature core protein, 191 amino acids in length, on the endoplasmic reticulum (ER) (16). This protein consists of three predicted domains: the N-terminal hydrophilic domain (D1), the C-terminal hydrophobic domain (D2), and the tail domain (33), which serves as a signal peptide for the E1 protein. D1 includes a number of positively charged amino acids responsible for viral RNA binding (amino acids 1 to 75) (43) and the region involved in multimerization of the core protein via homotypic interactions (amino acids 36 to 91 and 82 to 102) (32, 40) (see Fig. S1 in the supplemental material). Hydrophobic D2 includes the region responsible for core protein association with lipid droplets (LDs; amino acids 125 to 144) (7, 18, 37), which accumulate in response to core protein production (1, 6).

Many functions of the core protein have been reported (13, 38, 50), yet because infectious HCV particles cannot be appropriately produced in currently available experimental systems, HCV particle assembly has not been elucidated to date. A cell culture system that reproduces the complete life cycle of HCV *in vitro* was developed by Wakita et al. using a cloned HCV genome (JFH1) (53). Using this system, the assembly of infectious HCV particles was found to occur near LDs and ER-derived LD-associated membranes (36, 47). Neither the structures nor the functions of the virus proteins involved in virus particle assembly are known, however. To elucidate this point, we have analyzed the biochemical characteristics of the proteins within the fraction containing the HCV particle and found a disulfide-bonded core protein complex (dbc-complex). We revealed that the disulfide-bonded dimer of core protein (dbd-core) was formed by a single cysteine residue at amino

* Corresponding author. Mailing address: Department of Viral Oncology, Institute for Virus Research, Kyoto University, 53 Kawahara-cho Shougoin, Kyoto 606-8507, Japan. Phone: 81-75-751-4046. Fax: 81-75-751-3998. E-mail: mhijikat@virus.kyoto-u.ac.jp.

† Supplemental material for this article may be found at http://jvi.asm.org/.

▽ Published ahead of print on 30 June 2010.

acid position 128 on the ER. The roles of the disulfide bond of the core protein in virus-like particle formation are discussed in this paper.

MATERIALS AND METHODS

Cell culture. Cells of the HuH-7 and HuH-7.5 human hepatoma cell lines were grown in Dulbecco's modified Eagle's medium (Nacalai Tesque, Kyoto, Japan) supplemented with 10% fetal bovine serum, 100 U/ml nonessential amino acids (Invitrogen, Carlsbad, CA), and 100 μg/ml each penicillin and streptomycin sulfate (Invitrogen).

Antibodies. The antibodies used for immunoblotting and indirect immunofluorescence analysis were specific for core protein (antibody 32-1), FLAG M2 (Sigma-Aldrich, St. Louis, MO), c-myc (Sigma-Aldrich), NS5A protein (CL1), adipocyte differentiation-related protein (ADRP; StressGen, Victoria, British, Columbia, Canada), calnexin (Calnexin-NT; StressGen), and glyceraldehyde-3-phosphate dehydrogenase (GAPDH; Chemicon, Temecula, CA). Antibodies specific for core protein (antibody 32-1) were a gift from M. Kohara (The Tokyo Metropolitan Institute of Medical Science, Tokyo, Japan). Rabbit polyclonal anti-NS5A protein CL1 antibodies have been described previously (36).

Plasmid construction. All plasmids were generated by inserting PCR-amplified fragments into expression plasmids. The plasmids, primer sequences, templates for the PCRs, and restriction enzyme sites used to construct the plasmids are listed in Table S1 in the supplemental material. Plasmids pJFH1^{E2FL} (encoding the full-length HCV genome with the FLAG epitope in the E2 hypervariable region), pJFH1^{AAA99} (encoding a NS5A mutant of JFH1^{E2FL}, resulting in noninfectious HCV particles), pJFH1$^{PP/AA}$ (encoding a core protein mutant of JFH1^{E2FL}, which allows replication in cells but prevents HCV particle production), and pcDNA3-core^{WT} (an expression plasmid encoding the full-length core protein of JFH1) have been described previously (36). Plasmid pJ6/JFH1, which contains the full-length HCV genome encoding structural proteins from the J6 strain and nonstructural proteins from the JFH1 strain, was kindly provided by Charles M. Rice (The Rockefeller University, New York, NY).

***In vitro* transcription.** RNA for transfection was synthesized as described previously (36). In brief, plasmids carrying the HCV RNA sequence were linearized with XbaI and used as templates for *in vitro* transcription with MEGAscript T7 (Ambion, Austin, TX).

Transfection. Ten micrograms of JFH1^{E2FL}, JFH1^{C128A}, JFH1^{C184A}, JFH1$^{C128/184A}$, JFH1$^{PP/AA}$, or JFH^{AAA99} and J6/JFH1 or J6/JFH1^{AAA99} RNAs were transfected into HuH-7 and HuH-7.5 cells (1.0×10^7 cells) by electroporation (260 V, 0.95 μF) using a Gene Pulser II system (Bio-Rad, Hercules, CA). Core protein expression plasmids were transfected into HuH-7 cells using Lipofectamine LTX (Invitrogen), according to the manufacturer's protocol.

HCV particle precipitation. Culture medium from HCV RNA-transfected cells were concentrated using Amicon Ultra-15 centrifugal filters with Ultracell-100 membranes (Millipore, Billerica, MA) and mixed with sucrose solution in phosphate-buffered saline (PBS) to a final sucrose concentration of 2%. This mixture was ultracentrifuged (100,000 × *g*, 4°C for 2 h), and the HCV particles were obtained as a pellet. The pellet was then suspended in culture medium for infection experiments or PBS for immunoblot analysis.

Indirect immunofluorescence analysis. Indirect immunofluorescence analyses of HCV infection and the cellular localization of the HCV proteins were performed as described previously (36).

Protease protection assay. Concentrated culture medium from JFH1^{E2FL} RNA-transfected HuH-7 cells was fractionated using 20 to 50% sucrose density gradients, and the HCV RNA titer was measured in quantitative reverse transcription-PCRs (RT-PCRs) as described below. Fractions with high HCV RNA titers were collected, and JFH1^{E2FL} particles were obtained as a pellet after ultracentrifugation (100,000 × *g*, 4°C for 2 h). The pellet was suspended in PBS and treated with 10 μg/ml trypsin or 5 μg/ml proteinase K in the presence or absence of 1% Nonidet P-40 (NP-40) at 37°C for 15 min, unless otherwise indicated. The reaction was quenched by the addition of protease inhibitor cocktail (Nacalai Tesque), followed by SDS-PAGE under nonreducing conditions and immunoblotting specific for core protein.

Immunoblot analysis. Samples were subjected to SDS-PAGE in sample buffer (62.5 mM Tris-HCl [pH 7.8], 1% SDS, 10% glycerol) with or without 5% β-mercaptoethanol (β-ME) or 50 mM dithiothreitol (DTT) for reducing and nonreducing conditions, respectively. *N*-Ethylmaleimide (NEM; Nacalai Tesque) was added to the sample buffer to a final concentration of 5 mM for the indicated samples. Proteins were transferred to a polyvinylidene difluoride membrane and blocked in blocking buffer for 1 h at room temperature with gentle agitation. After incubation with primary antibodies overnight at 4°C, the membrane was washed three times for 5 min in washing buffer at room temperature with gentle agitation. The membrane was then incubated with horseradish peroxidase (HRP)-conjugated secondary antibodies for 1 h at room temperature. After three washes in washing buffer, proteins were detected using Western Lightning reagent (PerkinElmer, Waltham, MA) or ECL Advance (GE Healthcare, Buckinghamshire, England) and Kodak MXJB Plus medical X-ray film (Kodak, Rochester, NY) or an LAS-4000 system (Fujifilm, Tokyo, Japan).

Preparation of LDs. LDs were prepared as described previously (36).

Preparation of MMFs. Microsomal membrane fractions (MMFs) were collected as described previously (15) with some modifications. In brief, cells were collected in homogenization buffer (20 mM Tris-HCl [pH 7.8], 250 mM sucrose, and 0.1% ethanol supplemented with protease inhibitor cocktail) and homogenized on ice using 40 strokes of a Dounce homogenizer. The samples were then centrifuged at 1,000 × *g* for 10 min at 4°C. The supernatant was collected in a new tube and centrifuged again at 16,000 × *g* for 20 min at 4°C. The supernatant was further centrifuged at 100,000 × *g* for 1 h at 4°C. The MMF precipitate was homogenized in lysis buffer (1% NP-40, 0.1% SDS, 20 mM Tris-HCl [pH 8.0], 150 mM NaCl, 1 mM EDTA, and 10% glycerol supplemented with protease inhibitor cocktail) using a Dounce homogenizer.

qRT-PCR analysis. Quantitative RT-PCR (qRT-PCR) analysis for determination of the HCV RNA titer was performed as described previously (36).

ELISA specific for core protein. The core protein in culture medium was quantified using an enzyme-linked immunosorbent assay (ELISA; HCV antigen ELISA; Ortho-Clinical Diagnostics, Raritan, NJ), according to the manufacturer's protocol.

RNA-protein binding precipitation assay. Core^{WT} or core^{C128A} was translated *in vitro* from pcDNA3-core^{WT} and pcDNA3-core^{C128A}, respectively, using a TNT-coupled rabbit reticulocyte lysate system (Promega, Madison, WI), according to the manufacturer's protocol. These proteins were incubated with poly(U) agarose (Sigma) in binding buffer (50 mM HEPES (pH 7.4)–100 mM NaCl–0.1% NP-40–20 U RNase inhibitor) at 4°C for 2 h with or without RNase A. After five washes, the resin-bound core proteins were immunoblotted.

RESULTS

The HCV particle contains core protein complex formed by a disulfide bond. To analyze the core protein of the HCV particle, we first subjected the concentrated culture medium of HuH-7 cells transfected with *in vitro*-transcribed JFH1^{E2FL} RNA to ultracentrifugation. After the resulting pellet was resuspended in culture medium, we confirmed the presence of infectious HCV particles on the basis of the infectivity of HuH-7.5 cells (Fig. 1a). The infectious JFH1^{E2FL} particle-containing pellet was separated by SDS-PAGE under nonreducing conditions, and immunoblot analysis showed the presence of a core antibody-reactive protein that was approximately twice the size of the core protein (38 kDa), in addition to the expected 19-kDa core protein (Fig. 1b, lane 1). Because treatment with DTT eliminated the larger core protein antibody-reactive band while the levels of the core protein monomer increased (Fig. 1b, lanes 2 to 6), the larger protein likely represented a dbc-complex. This complex was also found in J6/JFH1-derived particles (see Fig. S2 in the supplemental material), indicating that the complex was not specific for JFH1^{E2FL}.

To determine whether the dbc-complex is a component of the HCV particle, a protease protection assay was performed using RNase-resistant HCV particles fractionated on the basis of their buoyant densities. Concentrated culture medium from HuH-7 cells transfected with *in vitro*-transcribed JFH1^{E2FL} RNA was fractionated using a 20 to 50% sucrose density gradient; and JFH1^{E2FL} particles, which were presumed to contain both infectious and noninfectious particles, were collected from fractions with high HCV RNA titers using ultracentrifugation (Fig. 2a, fractions 8 to 13). The core protein from the collected fractions was analyzed by immunoblotting after SDS-

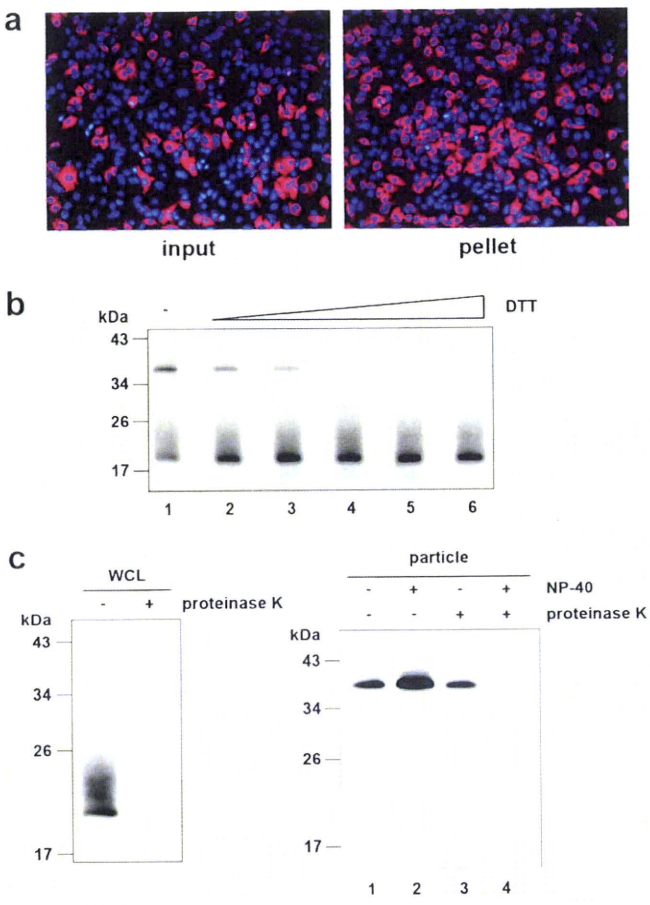

FIG. 1. The HCV-like particle consists of a core complex formed by a disulfide bond. (a) The infectivity of the pellet fraction collected from concentrated culture medium from JFH1^{E2FL} RNA-transfected HuH-7 cells was analyzed as described in Materials and Methods. Input indicates the same volume of concentrated culture medium used to pellet the virus-like particles. (b) Immunoblot analysis of the core protein in pellets containing JFH1^{E2FL} virus particles treated with various levels of DTT (lanes 1, 2, 3, 4, 5, and 6, 0, 1.56, 3.13, 6.25, 12.5, and 25 mM DTT, respectively). (c) Immunoblot analysis of the core protein in JFH1^{E2FL} particles collected from sucrose density gradient fractions with high HCV RNA titers (particle) (Fig. 2a, fractions 8 to 13) and treated with 5 μg/ml proteinase K at 37°C for 15 min in the presence or absence of 1% NP-40 (right panel). As a positive control, WCL prepared from JFH1^{E2FL} RNA-transfected HuH-7 cells in lysis buffer was treated with 5 μg/ml proteinase K at 37°C for 15 min (left panel). Data are representative of three independent experiments.

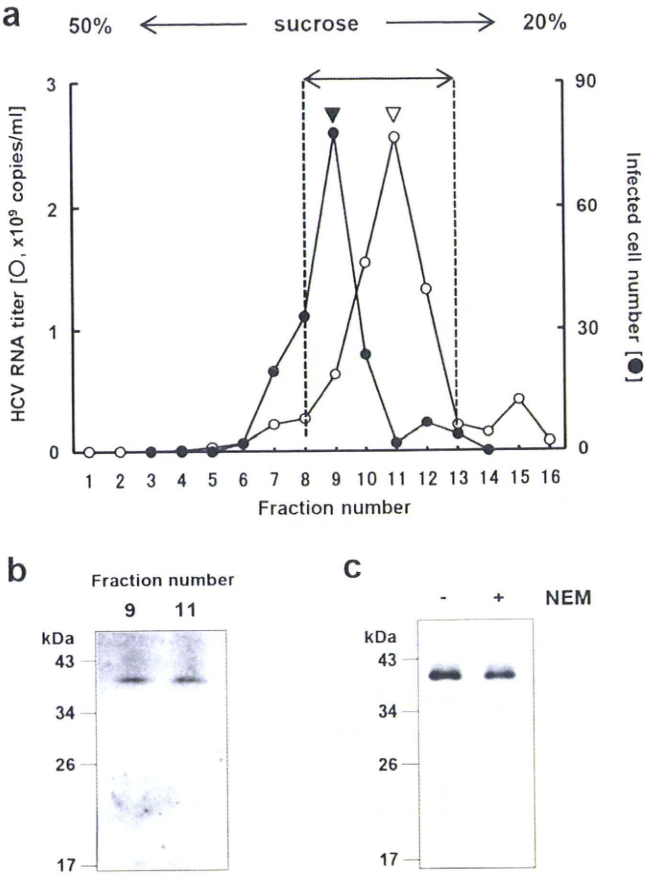

FIG. 2. HCV nucleocapsid-like particle consists of core complex. (a) HCV RNA titer in culture medium separated on a 20 to 50% sucrose density gradient. Concentrated culture medium from JFH1^{E2FL} RNA-transfected HuH-7 cells were treated with RNase and separated on a 20 to 50% sucrose density gradient. Fractions 1 to 16 were obtained from the bottom to the top of the tube, respectively. The HCV RNA titer and infectivity of each fraction were analyzed by real-time qRT-PCR (for fractions 1 to 16) and counting the number of cells infected with HCV-like particle detected by immunofluorescence (for fractions 3 to 14), respectively, as described in Materials and Methods. In brief, each fraction was diluted with 1× PBS and HCV-like particles were collected by ultracentrifugation, and then the pellets were suspended in culture medium and used for infection. (b) HCV-like particle collected from the infectious HCV peak (from panel a, filled arrowhead) and the HCV RNA peak (from panel a, open arrowhead) were collected by ultracentrifugation, subjected to nonreducing SDS-PAGE, and detected by immunoblotting against the core protein. (c) HCV-like particles collected from fractions 8 to 13 (a) were subjected to nonreducing SDS-PAGE in the presence (lane +) or absence (lane −) of 5 mM NEM and analyzed by immunoblotting against the core protein. Data are representative of two (a, infectivity of fractions) or three independent experiments.

PAGE under nonreducing conditions and showed only the dbc-complex (Fig. 1c, right panel).

To examine whether the complex contributes to the infectivity of the particles, we analyzed the dbc-complex in the fractions containing infectious and noninfectious HCV particles (fractions 9 and 11 of Fig. 2a, filled and open arrowheads, respectively). Both the infectious and noninfectious HCV particle-containing fractions contained the dbc-complex (Fig. 2b). To confirm this further, a pellet containing particles of mutant JFH1^{AAA99}—a mutant of JFH1^{E2FL} that primarily produces noninfectious particles (36)—was analyzed in a similar manner. These dbc-complexes were found in pelleted particles of both JFH1^{AAA99} and J6/JFH1^{AAA99}, which was a mutant J6/JFH1 with a similar substitution to JFH1^{AAA99} (see Fig. S2 in the supplemental material). These results indicated that the dbc-complex was present in both the infectious and noninfectious HCV-like particles.

The core protein monomer observed in the pellet samples (Fig. 1b) may be from the secreted core protein or the debris of apoptotic cells, because the core protein is known to be secreted from cells expressing this protein under particular conditions (42) and strain JFH1 is known to cause apoptosis (45). The dbc-complex-specific signals in the HCV particles seem to be increased in the NP-40-treated samples for some

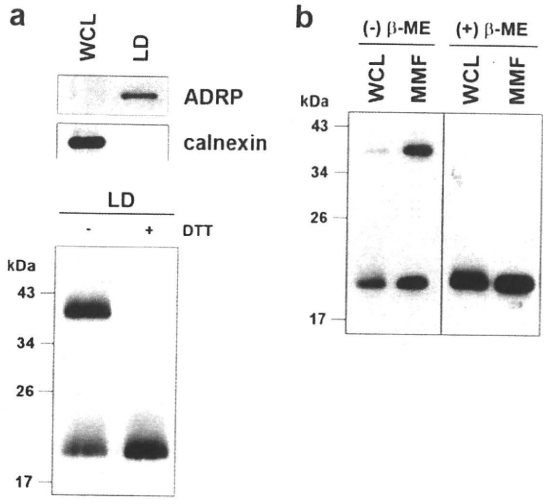

FIG. 3. The core complex is formed at the LD and ER. (a) The LD fraction and WCL were collected from JFH1^{E2FL} RNA-transfected HuH-7 cells on day 5 posttransfection. (upper panel) Immunoblot analysis of the LD marker ADRP and the ER marker calnexin in the LD fraction; (lower panel) immunoblot analysis of the core protein in the LD fraction treated or not treated with 50 mM DTT. (b) Immunoblot analysis of the core protein in the MMF and WCL collected from JFH1^{E2FL}-producing HuH-7 cells on day 5 posttransfection in the presence or absence of 5% β-ME. Data are representative of those from three independent experiments.

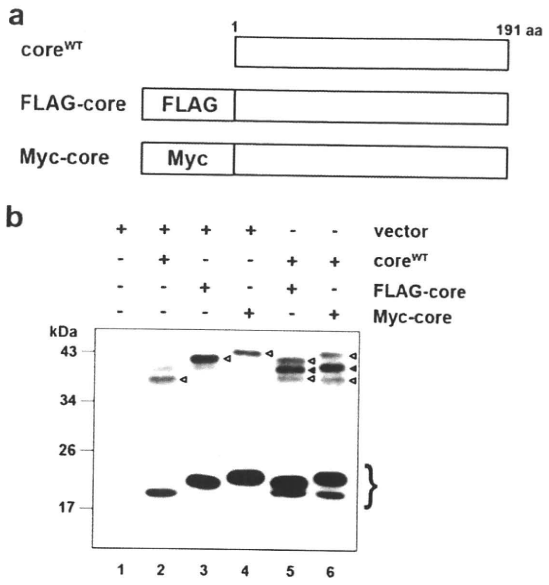

FIG. 4. The core complex consists of a core dimer. (a) Schematic of wild-type, FLAG-tagged (FLAG-core), and Myc-tagged (Myc-core) core proteins. (b) Immunoblot analysis of the core protein in the MMF collected from HuH-7 cells transfected with combinations of pcDNA3 (vector) and/or core expression plasmids (e.g., encoding core^{WT}, FLAG-core, and Myc-core), as indicated. The experiment was performed under nonreducing conditions. The lower bands represent core monomer (marked on the right with a brace). White arrowheads, bands corresponding to dbd-core; black arrowheads, positions of the intermediately sized core complex formed by core^{WT} and the tagged core. Data are representative of those from three independent experiments.

unknown reason (Fig. 1c, lanes 1 and 2). Although the intermolecular disulfide bond is known to be artificially formed in denaturing SDS-PAGE in the absence of reducing agents, the dbc-complex was still observed even in the presence of NEM, which is the alkylating agent for free sulfhydryls, during sample preparation (Fig. 2c), indicating that the dbc-complex was naturally present in the virus-like particles.

The HCV nucleocapsid is covered with lipid membranes and E1 and E2 proteins, making it resistant to proteases. As expected, in the absence of NP-40, the dbc-complex was resistant to proteinase K (Fig. 1c, lane 3), whereas proteinase K was able to digest core protein in whole-cell lysates (WCLs) collected from JFH1^{E2FL}-transfected HuH-7 cells (Fig. 1c, left panel). Disrupting the envelope structure with NP-40 made the dbc-complex susceptible to proteinase K treatment (Fig. 1c, lane 4), indicating that the dbc-complex was indeed a component of the HCV particle.

The dbc-complex forms on the ER. To investigate the subcellular site at which the dbc-complex forms, LDs and MMFs from JFH1^{E2FL} replicating HuH-7 cells were analyzed by immunoblotting. We first analyzed the dbc-complex in LDs, because LDs are involved in infectious HCV particle formation (36, 47). The purity of the LD fraction was determined using immunoblot analysis of calnexin and ADRP, ER and LD marker proteins, respectively (Fig. 3a, upper panel). The core protein was then analyzed in the LD fraction. As shown in Fig. 3a (lower panel), the dbc-complex was observed in the LD fraction from JFH1^{E2FL} RNA-transfected HuH-7 cells. We next analyzed the core protein in the ER-containing MMF, because the core protein is first translated and processed on the ER (16). As shown in Fig. 3b, the dbc-complex was observed in the MMF from JFH1^{E2FL} RNA-transfected HuH-7 cells. These results suggest that the dbc-complex is first formed at the ER. To assess the possibility that dbc-complex-containing HCV particles were also assembled on the ER, the sensitivity of the dbc-complex to protease treatment was analyzed. The dbc-complex in the MMF was susceptible to protease treatment in the absence of NP-40, indicating that the dbc-complex on the ER was not yet part of a HCV particle (data not shown).

dbc-complex is most likely a disulfide-bonded dimer form of the core. In order to examine whether the core protein itself has the potential to form a dbc-complex, we analyzed the dbc-complex formation of the full-length wild-type core protein (core^{WT}) expressed from pcDNA3-core^{WT} (36), the expression plasmid encoding the 191-amino-acid full-length core protein of JFH1 strain. We used this expression plasmid because the core protein from this plasmid was likely to be processed correctly enough to produce infectious HCV particles when it was cotransfected with the RNA of JFH1^{dc3}, which is a core protein deletion mutant of JFH1 (36). As a result, the dbc-complex formation was observed from the MMF of core^{WT}-expressing cells both in the absence and in the presence of NEM (Fig. 4b; lane 2 and data not shown, respectively). We next investigated the effect of the amino acid region of E1 on the production of the dbc-complex, because it has been reported that the efficient processing of core protein is dependent on the presence of some E1 sequence to ensure the insertion of the signal sequence for E1 in the translocon/membrane machinery (34). The dbc-complex was also observed

when the core protein was expressed from pcDNA3-C-E1/25, which encodes the full-length core protein followed by the N-terminal 25-amino-acid sequence of E1 to ensure that the core protein is processed properly (see Fig. S3a in the supplemental material). These data showed that the dbc-complex was formed by expression of the core protein only in the cells.

Next, we examined the structural components of the dbc-complex. Because the dbc-complex was twice the size of the core protein monomer, it was likely dbd-core. So, we investigated whether the core protein molecules with different tags were able to form the dbd-core. We first generated expression plasmids encoding core protein with the N-terminal FLAG and Myc tags (pcDNA3-FLAG-core and pcDNA3-Myc-core, respectively; Fig. 4a). The tagged core proteins were expressed or coexpressed with $core^{WT}$ in HuH-7 cells, and the MMF was analyzed by immunoblotting. The FLAG or Myc tag shifted the positions of the monomer and the complex bands (Fig. 4b, lanes 3 and 4) compared with the position of $core^{WT}$ (Fig. 4b, lane 2). When $core^{WT}$ was coexpressed with FLAG-core or Myc-core, the core protein complex of an intermediate size was observed, in addition to the bands obtained when the constructs were independently expressed (Fig. 4b, lanes 5 and 6, filled arrowheads); the intermediate-sized band disappeared after treatment with β-ME (see Fig. S3b, lanes 11 and 12, filled arrows, in the supplemental material), indicating that $core^{WT}$ and tagged core protein formed a heteromeric disulfide-bonded dimer. These results demonstrated that the dbc-complex on the ER is a dbd-core. Although we tried to detect the hetero- or homodimer consisting of the tagged core protein by using anti-FLAG or anti-Myc antibodies, these dimers were not detected, possibly because of the lower levels of sensitivity and specificity of the antibodies compared to those of the anti-core protein antibody that we used, especially against epitopes in the dbd-core. The results presented above, coupled with the similarities of the molecular sizes and sensitivities to β-ME and DTT, suggested that the dbc-complex in the HCV particle is most likely a dbd-core.

Core protein Cys128 mediates dbd-core formation. Our results showed that core protein from $JFH1^{E2FL}$ forms a disulfide-bonded dimer on the ER. A search for cysteine residues in the $JFH1^{E2FL}$ core protein identified amino acid positions 128 (Cys128) and 184 (Cys184) (see Fig. S1 in the supplemental material). These residues are highly conserved in core proteins from the approximately 2,000 reported HCV strains (HCVdb, http://www.hcvdb.org/, Hepatitis C Virus Database; http://s2as02.genes.nig.ac.jp/). To determine which cysteine residue mediated disulfide bond formation, we generated point mutations in $JFH1^{E2FL}$ that replaced Cys128 and/or Cys184 with alanine (Ala) (C128A, C184A, and C128/184A in $JFH1^{C128A}$, $JFH1^{C184A}$, and $JFH1^{C128/184A}$, respectively; Fig. 5a). As shown in Fig. 5b, the core proteins from $JFH1^{C128A}$ and $JFH1^{C128/184A}$ failed to form a dbd-core under nonreducing condition, whereas the core protein from $JFH1^{C184A}$ formed the dimer, indicating that Cys128 was the residue responsible. Similar results were observed when Cys was replaced by serine (Ser) instead of Ala (see Fig. S5c in the supplemental material). Recently, Majeau et al. reported that the core protein of the J6/JFH1 strain with Cys128 replacements by Ala or Ser were unstable in both *Pichia pastoris* and human hepatoma cell line HuH-7.5 (31), although we did not detect any noticeable degradation of the mutant core proteins of strain JFH1 (Fig. 5b; see also Fig. S5c in the supplemental material). This difference may have resulted from the difference in sample preparation methods, as we used the full-length genome of $JFH1^{E2FL}$ strain bearing the strain JFH1 core protein and HuH-7 cells instead of a core protein-expressing plasmid for the J6 strain and HuH-7.5 cells.

To exclude the possibility that mutation of Cys128 inhibited dbd-core formation by creating a conformational change, T127A and G129A core protein mutants ($JFH1^{T127A}$ and $JHF1^{G129A}$, respectively) were created and examined for their effects on dbd-core formation and infectious virus particle production. These mutants formed dbd-core, and infectious HCV particles were detected in the culture medium (see Fig. S4a to c in the supplemental material), supporting an essential role for Cys128 in dbd-core and particle formation.

dbd-core contributes to HCV particle production. To examine the functional roles of dbd-core, infectious HCV particle production, HCV replication efficiency, colocalization of the core protein and LDs, and RNA binding of mutant and wild-type ($JFH1^{E2FL}$) core protein were evaluated. Culture medium from HuH-7 cells transfected with $JFH1^{C128A}$ or $JFH1^{C128/184A}$ RNA contained significantly fewer infectious HCV particles compared with the numbers obtained with $JFH1^{E2FL}$ or $JFH1^{C184A}$ RNA (Fig. 5c). We also found significant decreases in the levels of HCV RNA and core protein in the culture medium of HuH-7 cells transfected with $JFH1^{C128A}$ or $JFH1^{C128/184A}$ RNA (Fig. 5d and e). Similar results were observed with J6/JFH1 C128A or the C128/184A mutant strain (data not shown). To investigate whether these results were due to suppressed HCV replication, the HCV RNA and protein levels in cells transfected with mutant RNA were analyzed using qRT-PCR and immunoblot analyses, respectively. Compared with the results obtained with $JFH1^{E2FL}$, no significant changes in the cellular HCV RNA titer at days 1, 3, and 5 posttransfection or in the expression of HCV nonstructural protein NS5A were observed (Fig. 6a and b). This indicated that substitution of Cys128 did not significantly affect HCV RNA genome replication or viral protein production, demonstrating that the dbd-core functions during HCV particle production rather than HCV genome replication. Similar results were observed using RNA of JFH1 mutant strain $JFH1^{C128S}$, in which the cysteine at position 128 was replaced by Ser instead of Ala (see Fig. S5a, b, and d in the supplemental material).

The subcellular localizations of the core protein and NS5A protein in HuH-7 cells transfected with HCV RNA were investigated using indirect immunofluorescence and confocal microscopy, because recruiting HCV proteins to LDs is an important step in infectious HCV particle production (36, 47) and core trafficking to LDs is dependent on signal peptide peptidase (SPP)-mediated cleavage of the tail region (34, 41). $JFH1^{C128A}$ mutant core protein and NS5A protein were efficiently trafficked to LDs, as was observed with wild-type $JHF1^{E2FL}$ (Fig. 6c), suggesting that SPP cleavage and core protein maturation were not affected by the C128A mutation. Similar results were obtained with the core proteins derived from $JFH1^{C184A}$ and $JFH1^{C128/184A}$ (see Fig. S6 in the supplemental material) and also Ser mutant $JFH1^{C128S}$ (see Fig. 5e in the supplemental material).

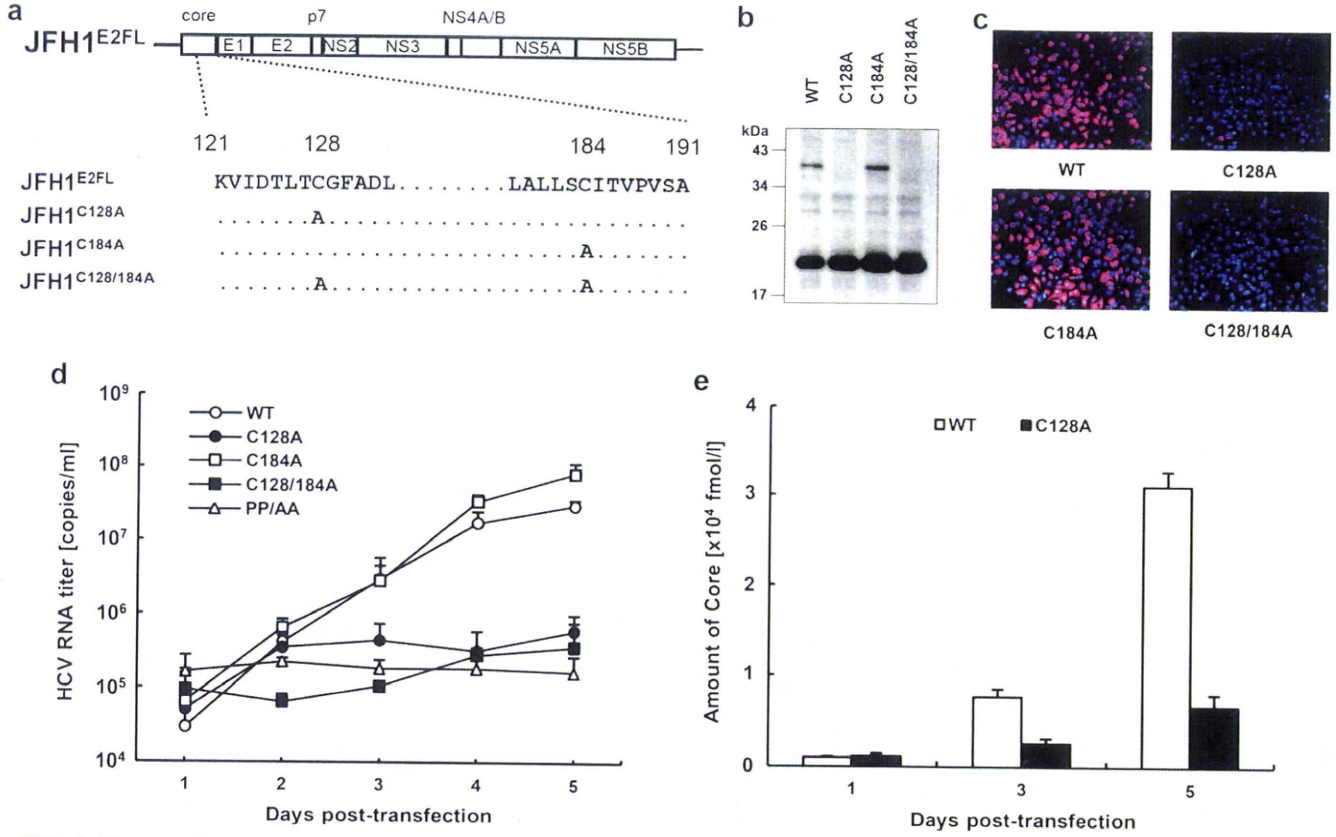

FIG. 5. The core dimer is formed via a bond between cysteine residues at amino acid position 128. (a) Site-directed mutagenesis of $JFH1^{E2FL}$. (b) Immunoblot analysis of the core protein in MMFs collected from HuH-7 cells under nonreducing conditions 3 days post-transfection with $JFH1^{E2FL}$ (WT), $JFH1^{C128A}$ (C128A), $JFH1^{C184A}$ (C184A), or $JFH1^{C128/184A}$ (C128/184A) RNA. (c) Infectivity of culture medium collected and concentrated on day 5 posttransfection from HuH-7 cells transfected with WT, C128A, C184A, or C128/184A RNA. (d) Real-time qRT-PCR analysis of HCV RNA titers in culture medium collected at the indicated time points from HuH-7 cells transfected with WT, C128A, C184A, C128/184A, or PP/AA ($JFH1^{PP/AA}$) RNA. (e) ELISAs of core protein levels in culture medium collected at the indicated time points from HuH-7 cells transfected with WT or C128A RNA. Data are representative of those from three independent experiments (b and c) or are the means ± standard deviations from three independent experiments (d and e).

Because HCV core protein can bind to RNA, including the HCV genome, during viral particle assembly (43), we analyzed RNA binding by the core protein using *in vitro*-translated $core^{C128A}$, $core^{WT}$, and poly(U) agarose resin. $Core^{C128A}$ and $core^{WT}$ bound similarly to the poly(U) resin (Fig. 6d).

dbd-core is important for HCV particle assembly. The mutational analysis of the core protein indicated that $core^{C128A}$ and $core^{WT}$ similarly localize to LDs, recruit NS proteins to the LD, and bind to RNA. Moreover, this mutation did not markedly affect HCV genome replication. How does $core^{C128A}$ affect the production of HCV particles? An important function of the core protein is multimerization, which is followed by capsid construction and packaging of the RNA genome in the viral particles. We therefore determined whether $core^{C128A}$ had a dominant negative effect on virus-like particle production. Wild-type $JFH1^{E2FL}$ RNA and different amounts of $JFH1^{C128A}$ RNA were cotransfected into HuH-7 cells, and the HCV RNA titer and infectivity of the virus-like particles in the culture medium were analyzed. As expected, the HCV RNA titer in the cells increased with higher levels of transfected RNA (see Fig. S7a in the supplemental material). In contrast, the HCV RNA titer and infectivity in the culture medium decreased in a $JFH1^{C128A}$ RNA dose-dependent manner when this mutant RNA was cotransfected with wild-type RNA (Fig. 7a, b). This suppressive effect was not observed when either wild-type RNA or core deletion mutant $JFH1^{dc3}$ RNA was used instead of mutant RNA in a similar experiment (see Fig. S7b to e in the supplemental material), indicating that higher levels of HCV RNA alone did not inhibit HCV particle production. Thus, $core^{C128A}$ had a dominant negative effect on HCV particle production. Together, these results suggest that dbd-core is involved in the assembly of HCV particles.

The nucleocapsid-like particle of HCV was resistant to trypsin treatment. To further investigate the structure of the HCV nucleocapsid-like particle most likely formed by dbd-core, we examined the sensitivity of the particle to trypsin, which cleaves polypeptides at the C-terminal end of basic residues. Whereas trypsin digested the core protein in the whole-cell lysates (Fig. 8a, left panel), dbd-core from buoyant density-fractionated $JFH1^{E2FL}$ particles was resistant to digestion, despite NP-40 treatment (Fig. 8a, right panel), although it was sensitive to proteinase K, which has a broad specificity (Fig. 1c). The N-terminal hydrophilic domain of the core protein (from residues 6 to 121) contains a number of trypsin cleavage sites (25 sites

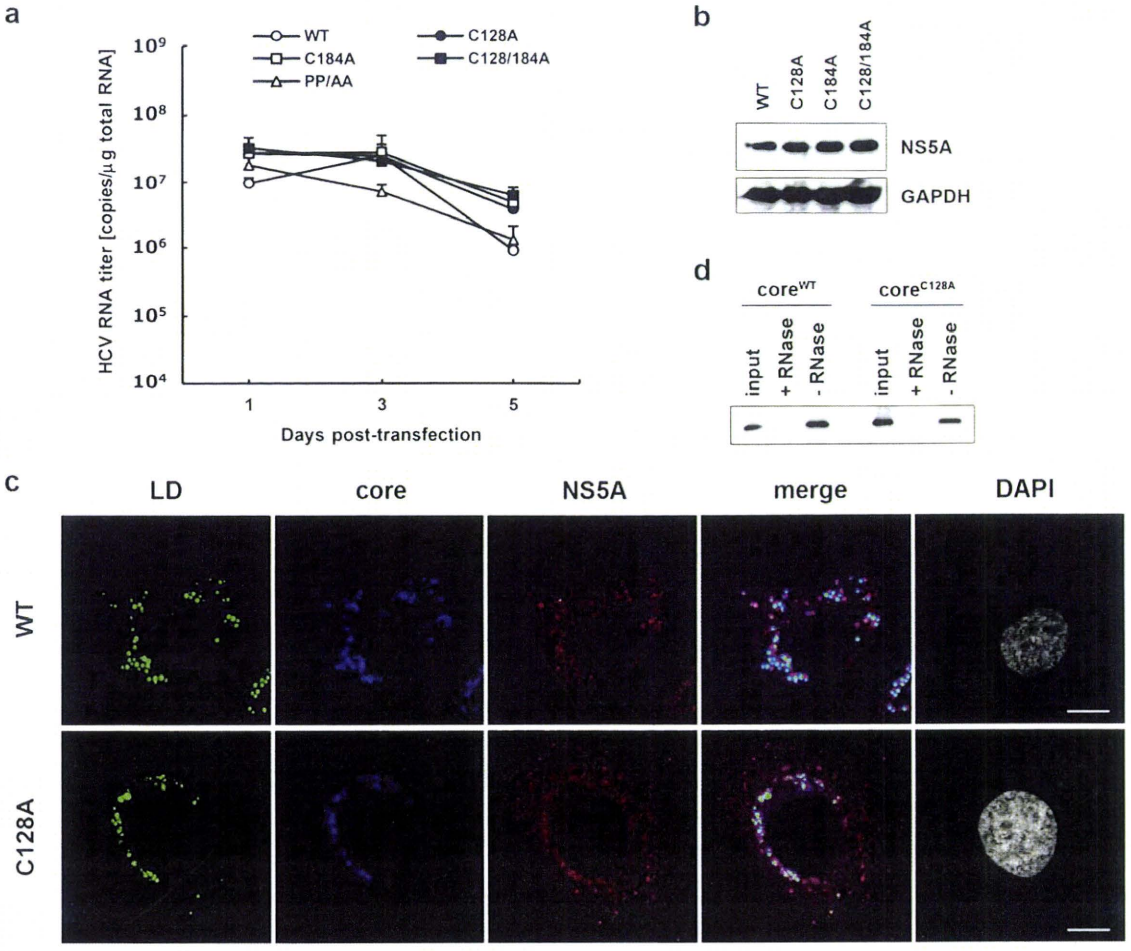

FIG. 6. Site-directed mutagenesis has no effect on HCV replication. (a) Real-time qRT-PCR analysis of the HCV RNA titer using total cellular RNA collected at the indicated time points from cells transfected with JFH1^{E2FL} (WT), JFH1^{C128A} (C128A), JFH1^{C184A} (C184A), JFH1$^{C128/184A}$ (C128/184A), or JFH1$^{PP/AA}$ (PP/AA) RNA. (b) Immunoblot analysis of NS5A protein and GAPDH in whole-cell lysate collected from cells transfected with WT, C128A, C184A, or C128/184A RNA at day 3 posttransfection. (c) Confocal microscopy of the subcellular localization of the LD (green), core (blue), NS5A protein (red), and nucleus (4′,6-diamidino-2-phenylindole [DAPI]) (gray) in WT and C128A replicating cells on day 3 posttransfection. Bars, 10 μm. (d) An RNA-protein binding precipitation assay was performed with *in vitro*-translated core^{WT} and core^{C128A} using poly(U) agarose as the resin. +RNase and −RNase, samples with and without RNase treatment, respectively, as described in Materials and Methods. Input indicates that 1/40 of the amount of translated product was used in this assay. Data represent the means ± standard deviations from three independent experiments (a) or are representative of those from three independent experiments (b to d).

in strain JHF1) (see Fig. S1 in the supplemental material), suggesting that the N-terminal domain faces inward and/or that the conformation prevents protease access. To address this idea, buoyant density-fractionated JFH1^{E2FL} particles were treated with trypsin under stricter conditions in the presence of NP-40. Cleavage of dbd-core by various levels of trypsin correlated with the appearance of a shorter molecule (Fig. 8b, white arrowhead). The shorter molecule was presumed to be partially digested dbd-core with an intact N-terminal region because it was recognized by anti-core protein antibodies, which bind to an epitope located from amino acids 20 to 40 of the core protein (M. Kohara, The Tokyo Metropolitan Institute of Medical Science, personal communication). These results suggest that dbd-core is assembled into the nucleocapsid-like particle such that most of the N-terminal domain is inside.

DISCUSSION

In the present study, we have shown that the nucleocapsid-like particle of HCV most likely contains a dimer of core protein that is stabilized by a disulfide bond. Mutational analysis revealed that Cys128 forms a disulfide bond between core monomers. Several reports have shown that disulfide bonds in the capsid proteins of some viruses are involved in virus particle assembly and stabilization of the viral capsid structure (4, 21, 27, 28, 57); these viruses are characterized by icosahedral nucleocapsids. Because, like these viruses, the HCV virion is spherical (2, 20), it has been suggested that HCV may contain a nucleocapsid with a similar structure (20). We found the dbc-complex, which is most likely to be the dbd-core in JFH1^{E2FL} virus-like particles (Fig. 1c and 8a). The dbd-core in the capsid structure was digested by proteinase K but not

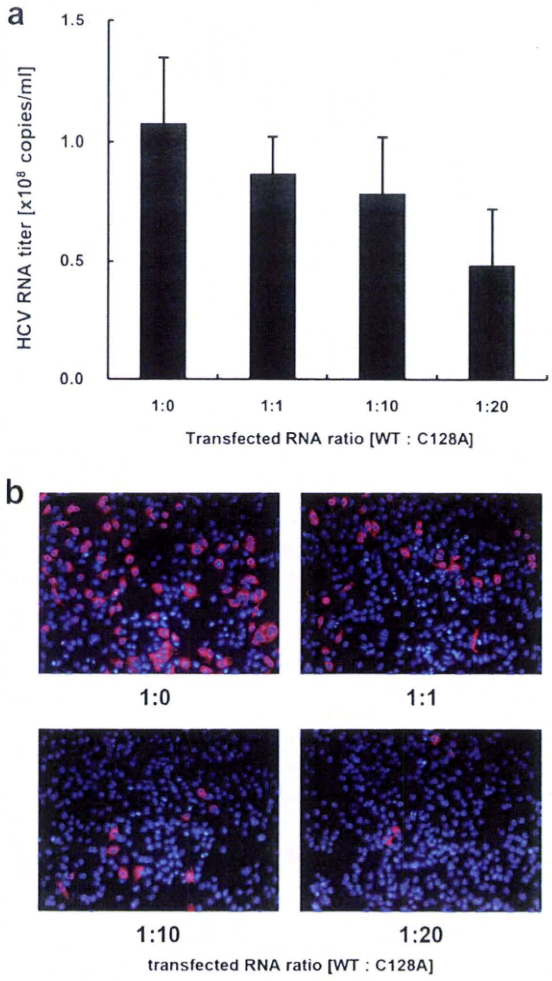

FIG. 7. JFH1^{C128A} core inhibits JFH1^{E2FL} particle assembly. A competitive inhibitory assay was performed with JFH1^{E2FL} (WT) and JFH1^{C128A} (C128A). (a) Real-time qRT-PCR analysis of the HCV RNA titer in HuH-7 cell culture medium 3 days after the cells were transfected with the indicated ratio of WT and C128A RNA. (b) The infectivity of culture medium collected from HuH-7 cells that had been transfected with the indicated ratio of WT and C128A RNA was analyzed as described in Materials and Methods. Data represent the means ± standard deviations from three independent experiments (a) or are representative of those from three independent experiments (b).

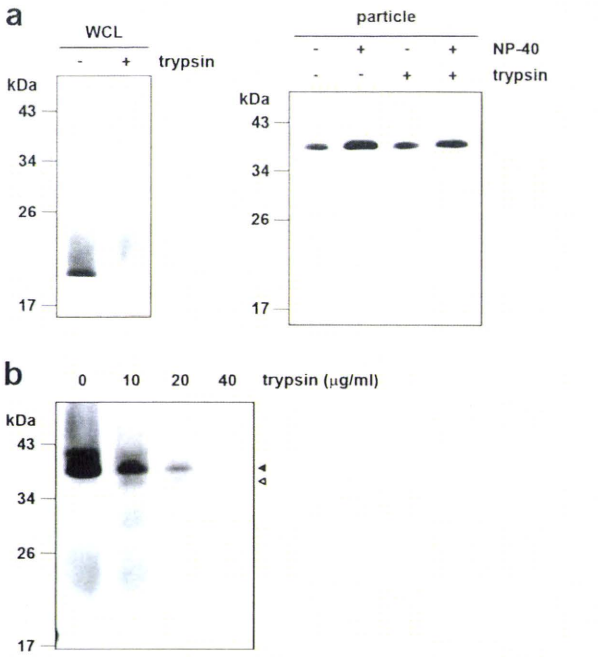

FIG. 8. The nucleocapsid-like particle of JFH1^{E2FL} is assembled with the C-terminal region of the core protein on the outer surface. (a) Immunoblot analysis of the core protein in JFH1^{E2FL} particles collected from sucrose density gradient fractions with high HCV RNA titers (particle) (Fig. 2a, fractions 8 to 13). The fractions were treated with 10 μg/ml trypsin at 37°C for 15 min in the presence or absence of 1% NP-40 (right panel). As a positive control, WCL prepared from JFH1^{E2FL} RNA-transfected HuH-7 cells in lysis buffer was treated with 10 μg/ml trypsin at 37°C for 15 min (left panel). (b) Immunoblot analysis of the core protein in JFH1^{E2FL} particles collected from sucrose density gradient fractions with high HCV RNA titers (Fig. 2a, fractions 8 to 13). The fractions were treated with the indicated concentrations of trypsin at 37°C for 10 min in the presence of 1% NP-40. Open and filled arrows indicate the positions of dbd-core and the trypsin-digested fragment, respectively. Data are representative of those from three independent experiments.

trypsin in the presence of NP-40 (Fig. 1c and 8a, lane 4). The resistance to trypsin suggested a tight conformation for dbd-core in the capsid and no exposed trypsin cleavage sites. The truncated form of dbd-core that was observed under certain trypsin treatment conditions likely resulted from cleavage in the C-terminal portion of the protein (e.g., arginine residues at positions 149 and 156) (see Fig. S1 in the supplemental material), although it is possible that the truncation of dbd-core was due to nonspecific cleavage by trypsin. These results imply that dbd-core is configured such that the N- and C-terminal ends are located at the inner and outer surfaces of the capsid, respectively. Because the N-terminal region of the core protein includes the RNA binding domain (43), the HCV RNA genome likely interacts with the core protein as it is packed in the nucleocapsid. On the other hand, the C-terminal hydrophobic domain probably faces the lipid membranes to form the envelope structure. Only part of the N-terminal hydrophilic region of the core protein has been structurally examined using X-ray crystal structural analysis (35) and structural bioinformatics and nuclear magnetic resonance analysis (11). Although the C-terminal half of the core protein has been structurally investigated by the use of bioinformatics (8), the three-dimensional structure containing the Cys128 residue is unknown. Thus, determination of the structure of the core protein in the nucleocapsid containing the Cys128 residue should be required for understanding the whole structure of this protein in the virus particles.

Because cotransfection of JFH1^{C128A} RNA with wild-type JFH1^{E2FL} RNA inhibited particle production in a mutant RNA dose-dependent manner (Fig. 7a and b), the C128A core variant clearly inhibited HCV particle formation by wild-type core protein. Cys128 was also previously reported to be a residue included in the region important for the production of infectious HCV (39). This residue is located near the N-terminal end of the hydrophobic region of the core (amino acids 122 to 177) and belongs to the hydrophilic side of an amphipathic helix expected to interact in the plane of the membrane interface (7). Therefore, it is possible to think that dbd-core

formation via Cys128 can stabilize the interaction between the core protein and the membranes. The N-terminal half of the core protein (amino acids 1 to 124) reportedly assembles into nucleocapsid-like particles in the presence of the 5′ UTR from HCV RNA (24), suggesting that some nucleocapsid-like particles may assemble via only homotypic interactions from the core protein. In addition to weak homotypic interactions, the HCV core protein forms a disulfide bond to stabilize the capsid structure, thus making dbd-core indispensable in the stable virus-like particle. We observed that culture medium from JFH1^{C128A}- or JFH1^{C128S}-transfected cells included slight infectivity (Fig. 5c; see also Fig. S5d in the supplemental material). This made us speculate that this mutant may produce some infective particle-like structure formed by a homotypic interaction of the core. Such a slight infectivity may have reflected the optimized *in vitro* culture conditions compared with the *in vivo* conditions, allowing relatively unstable virus particles to survive.

A nucleocapsid must be resistant to environmental degradation yet still be able to disassemble after infection. Disulfide bonds could help with this process by switching between a stable and unstable virus capsid on the basis of different intracellular and extracellular oxidation conditions (12, 30). During the virus life cycle, the disulfide bond strengthens the viral capsid structure and protects the viral genome from oxidative conditions and cellular nucleases when virus particles are formed. Upon infection, the disulfide bond may be cleaved under cytoplasmic reducing conditions, thereby releasing the viral genome into the cell for replication. HCV may utilize the core protein disulfide bond in this way as HCV enters the host cell via clathrin-mediated endocytosis (5) into a low-pH, endosomal compartment (25, 52); this is presumably followed by endosomal membrane fusion and release of the viral capsid into the cytoplasm (38).

Treatment of HCV infection with pegylated interferon in combination with ribavirin is not effective for all patients. Recently, drugs targeting viral proteins NS3/4A and NS5B have been examined in clinical trials. Although these drugs are relatively specific, resulting in fewer side effects and potent antiviral activity, monotherapy can be complicated by rapidly emerging resistant variants carrying mutations that reduce drug efficacy, perhaps due to conformational changes in the target (23, 48, 51). Therefore, viral proteins that are highly conserved among strains and those characterized by low mutation rates may be better targets for drug development. Because the core protein is the most conserved HCV protein and Cys128 is conserved among almost all HCV strains examined, drugs that interact with Cys128 and/or the region around or near this residue will likely show broad-spectrum efficacy to block stable infectious particle formation. Structural analysis of dbd-core should aid with the development of new STAT-Cs that target Cys128 by direct interaction with the sulfide group and/or region around this residue. Until now and still, the mechanism of disulfide bond formation of the core protein on the ER is unknown. Dimerization of the capsid protein by disulfide bond has been reported in some enveloped viruses (9, 19, 54, 56), although some were shown not to be important for virus particle formation (26, 55). Unlike vaccinia virus (46), no redox system of its own has been reported for these viruses. Therefore, further investigations addressing the mechanisms underlying dbd-core formation on the ER may reveal a new mechanism for disulfide bond formation of viral proteins in infected cells.

ACKNOWLEDGMENTS

This work was supported by grants-in-aid from the Ministry of Health, Labor, and Welfare of Japan and by grants-in-aid from the Japan Health Sciences Foundation.

REFERENCES

1. **Abid, K., V. Pazienza, A. de Gottardi, L. Rubbia-Brandt, B. Conne, P. Pugnale, C. Rossi, A. Mangia, and F. Negro.** 2005. An in vitro model of hepatitis C virus genotype 3a-associated triglycerides accumulation. J. Hepatol. **42**:744–751.
2. **Aly, H. H., Y. Qi, K. Atsuzawa, N. Usuda, Y. Takada, M. Mizokami, K. Shimotohno, and M. Hijikata.** 2009. Strain-dependent viral dynamics and virus-cell interactions in a novel in vitro system supporting the life cycle of blood-borne hepatitis C virus. Hepatology **50**:689–696.
3. **Asselah, T., Y. Benhamou, and P. Marcellin.** 2009. Protease and polymerase inhibitors for the treatment of hepatitis C. Liver Int. **29**(Suppl. 1):57–67.
4. **Baron, M. D., and K. Forsell.** 1991. Oligomerization of the structural proteins of rubella virus. Virology **185**:811–819.
5. **Blanchard, E., S. Belouzard, L. Goueslain, T. Wakita, J. Dubuisson, C. Wychowski, and Y. Rouille.** 2006. Hepatitis C virus entry depends on clathrin-mediated endocytosis. J. Virol. **80**:6964–6972.
6. **Boulant, S., M. W. Douglas, L. Moody, A. Budkowska, P. Targett-Adams, and J. McLauchlan.** 2008. Hepatitis C virus core protein induces lipid droplet redistribution in a microtubule- and dynein-dependent manner. Traffic **9**:1268–1282.
7. **Boulant, S., R. Montserret, R. G. Hope, M. Ratinier, P. Targett-Adams, J. P. Lavergne, F. Penin, and J. McLauchlan.** 2006. Structural determinants that target the hepatitis C virus core protein to lipid droplets. J. Biol. Chem. **281**:22236–22247.
8. **Boulant, S., C. Vanbelle, C. Ebel, F. Penin, and J. P. Lavergne.** 2005. Hepatitis C virus core protein is a dimeric alpha-helical protein exhibiting membrane protein features. J. Virol. **79**:11353–11365.
9. **Cornillez-Ty, C. T., and D. W. Lazinski.** 2003. Determination of the multimerization state of the hepatitis delta virus antigens in vivo. J. Virol. **77**:10314–10326.
10. **Dustin, L. B., and C. M. Rice.** 2007. Flying under the radar: the immunobiology of hepatitis C. Annu. Rev. Immunol. **25**:71–99.
11. **Duvignaud, J. B., C. Savard, R. Fromentin, N. Majeau, D. Leclerc, and S. M. Gagne.** 2009. Structure and dynamics of the N-terminal half of hepatitis C virus core protein: an intrinsically unstructured protein. Biochem. Biophys. Res. Commun. **378**:27–31.
12. **Freedman, R. B., B. E. Brockway, and N. Lambert.** 1984. Protein disulphide-isomerase and the formation of native disulphide bonds. Biochem. Soc. Trans. **12**:929–932.
13. **Giannini, C., and C. Brechot.** 2003. Hepatitis C virus biology. Cell Death Differ. **10**(Suppl. 1):S27–S38.
14. **Grakoui, A., C. Wychowski, C. Lin, S. M. Feinstone, and C. M. Rice.** 1993. Expression and identification of hepatitis C virus polyprotein cleavage products. J. Virol. **67**:1385–1395.
15. **Higashi, Y., H. Itabe, H. Fukase, M. Mori, Y. Fujimoto, R. Sato, T. Imanaka, and T. Takano.** 2002. Distribution of microsomal triglyceride transfer protein within sub-endoplasmic reticulum regions in human hepatoma cells. Biochim. Biophys. Acta **1581**:127–136.
16. **Hijikata, M., N. Kato, Y. Ootsuyama, M. Nakagawa, and K. Shimotohno.** 1991. Gene mapping of the putative structural region of the hepatitis C virus genome by in vitro processing analysis. Proc. Natl. Acad. Sci. U. S. A. **88**:5547–5551.
17. **Hijikata, M., H. Mizushima, Y. Tanji, Y. Komoda, Y. Hirowatari, T. Akagi, N. Kato, K. Kimura, and K. Shimotohno.** 1993. Proteolytic processing and membrane association of putative nonstructural proteins of hepatitis C virus. Proc. Natl. Acad. Sci. U. S. A. **90**:10773–10777.
18. **Hope, R. G., and J. McLauchlan.** 2000. Sequence motifs required for lipid droplet association and protein stability are unique to the hepatitis C virus core protein. J. Gen. Virol. **81**:1913–1925.
19. **Hu, H. M., K. N. Shih, and S. J. Lo.** 1996. Disulfide bond formation of the in vitro-translated large antigen of hepatitis D virus. J. Virol. Methods **60**:39–46.
20. **Ishida, S., M. Kaito, M. Kohara, K. Tsukiyama-Kohora, N. Fujita, J. Ikoma, Y. Adachi, and S. Watanabe.** 2001. Hepatitis C virus core particle detected by immunoelectron microscopy and optical rotation technique. Hepatol. Res. **20**:335–347.
21. **Jeng, K. S., C. P. Hu, and C. M. Chang.** 1991. Differential formation of disulfide linkages in the core antigen of extracellular and intracellular hepatitis B virus core particles. J. Virol. **65**:3924–3927.
22. **Kato, N., M. Hijikata, Y. Ootsuyama, M. Nakagawa, S. Ohkoshi, T. Sug-**

imura, and K. Shimotohno. 1990. Molecular cloning of the human hepatitis C virus genome from Japanese patients with non-A, non-B hepatitis. Proc. Natl. Acad. Sci. U. S. A. **87:**9524–9528.
23. **Kieffer, T. L., A. D. Kwong, and G. R. Picchio.** 2010. Viral resistance to specifically targeted antiviral therapies for hepatitis C (STAT-Cs). J. Antimicrob. Chemother. **65:**202–212.
24. **Kim, M., Y. Ha, and H. J. Park.** 2006. Structural requirements for assembly and homotypic interactions of the hepatitis C virus core protein. Virus Res. **122:**137–143.
25. **Koutsoudakis, G., A. Kaul, E. Steinmann, S. Kallis, V. Lohmann, T. Pietschmann, and R. Bartenschlager.** 2006. Characterization of the early steps of hepatitis C virus infection by using luciferase reporter viruses. J. Virol. **80:**5308–5320.
26. **Lee, J. Y., D. Hwang, and S. Gillam.** 1996. Dimerization of rubella virus capsid protein is not required for virus particle formation. Virology **216:**223–227.
27. **Li, M., P. Beard, P. A. Estes, M. K. Lyon, and R. L. Garcea.** 1998. Intercapsomeric disulfide bonds in papillomavirus assembly and disassembly. J. Virol. **72:**2160–2167.
28. **Li, P. P., A. Nakanishi, S. W. Clark, and H. Kasamatsu.** 2002. Formation of transitory intrachain and interchain disulfide bonds accompanies the folding and oligomerization of simian virus 40 Vp1 in the cytoplasm. Proc. Natl. Acad. Sci. U. S. A. **99:**1353–1358.
29. **Liang, T. J., L. J. Jeffers, K. R. Reddy, M. De Medina, I. T. Parker, H. Cheinquer, V. Idrovo, A. Rabassa, and E. R. Schiff.** 1993. Viral pathogenesis of hepatocellular carcinoma in the United States. Hepatology **18:**1326–1333.
30. **Liljas, L.** 1999. Virus assembly. Curr. Opin. Struct. Biol. **9:**129–134.
31. **Majeau, N., R. Fromentin, C. Savard, M. Duval, M. J. Tremblay, and D. Leclerc.** 2009. Palmitoylation of hepatitis C virus core protein is important for virion production. J. Biol. Chem. **284:**33915–33925.
32. **Matsumoto, M., S. B. Hwang, K. S. Jeng, N. Zhu, and M. M. Lai.** 1996. Homotypic interaction and multimerization of hepatitis C virus core protein. Virology **218:**43–51.
33. **McLauchlan, J.** 2000. Properties of the hepatitis C virus core protein: a structural protein that modulates cellular processes. J. Viral Hepat. **7:**2–14.
34. **McLauchlan, J., M. K. Lemberg, G. Hope, and B. Martoglio.** 2002. Intramembrane proteolysis promotes trafficking of hepatitis C virus core protein to lipid droplets. EMBO J. **21:**3980–3988.
35. **Menez, R., M. Bossus, B. H. Muller, G. Sibai, P. Dalbon, F. Ducancel, C. Jolivet-Reynaud, and E. A. Stura.** 2003. Crystal structure of a hydrophobic immunodominant antigenic site on hepatitis C virus core protein complexed to monoclonal antibody 19D9D6. J. Immunol. **170:**1917–1924.
36. **Miyanari, Y., K. Atsuzawa, N. Usuda, K. Watashi, T. Hishiki, M. Zayas, R. Bartenschlager, T. Wakita, M. Hijikata, and K. Shimotohno.** 2007. The lipid droplet is an important organelle for hepatitis C virus production. Nat. Cell Biol. **9:**1089–1097.
37. **Moradpour, D., C. Englert, T. Wakita, and J. R. Wands.** 1996. Characterization of cell lines allowing tightly regulated expression of hepatitis C virus core protein. Virology **222:**51–63.
38. **Moradpour, D., F. Penin, and C. M. Rice.** 2007. Replication of hepatitis C virus. Nat. Rev. Microbiol. **5:**453–463.
39. **Murray, C. L., C. T. Jones, J. Tassello, and C. M. Rice.** 2007. Alanine scanning of the hepatitis C virus core protein reveals numerous residues essential for production of infectious virus. J. Virol. **81:**10220–10231.
40. **Nolandt, O., V. Kern, H. Muller, E. Pfaff, L. Theilmann, R. Welker, and H. G. Krausslich.** 1997. Analysis of hepatitis C virus core protein interaction domains. J. Gen. Virol. **78**(Pt 6)**:**1331–1340.
41. **Okamoto, K., Y. Mori, Y. Komoda, T. Okamoto, M. Okochi, M. Takeda, T. Suzuki, K. Moriishi, and Y. Matsuura.** 2008. Intramembrane processing by signal peptide peptidase regulates the membrane localization of hepatitis C virus core protein and viral propagation. J. Virol. **82:**8349–8361.
42. **Sabile, A., G. Perlemuter, F. Bono, K. Kohara, F. Demaugre, M. Kohara, Y. Matsuura, T. Miyamura, C. Brechot, and G. Barba.** 1999. Hepatitis C virus core protein binds to apolipoprotein AII and its secretion is modulated by fibrates. Hepatology **30:**1064–1076.
43. **Santolini, E., G. Migliaccio, and N. La Monica.** 1994. Biosynthesis and biochemical properties of the hepatitis C virus core protein. J. Virol. **68:**3631–3641.
44. **Seeff, L. B., and J. H. Hoofnagle.** 2003. Appendix: The National Institutes of Health Consensus Development Conference Management of Hepatitis C 2002. Clin. Liver Dis. **7:**261–287.
45. **Sekine-Osajima, Y., N. Sakamoto, K. Mishima, M. Nakagawa, Y. Itsui, M. Tasaka, Y. Nishimura-Sakurai, C. H. Chen, T. Kanai, K. Tsuchiya, T. Wakita, N. Enomoto, and M. Watanabe.** 2008. Development of plaque assays for hepatitis C virus-JFH1 strain and isolation of mutants with enhanced cytopathogenicity and replication capacity. Virology **371:**71–85.
46. **Senkevich, T. G., C. L. White, E. V. Koonin, and B. Moss.** 2000. A viral member of the ERV1/ALR protein family participates in a cytoplasmic pathway of disulfide bond formation. Proc. Natl. Acad. Sci. U. S. A. **97:**12068–12073.
47. **Shavinskaya, A., S. Boulant, F. Penin, J. McLauchlan, and R. Bartenschlager.** 2007. The lipid droplet binding domain of hepatitis C virus core protein is a major determinant for efficient virus assembly. J. Biol. Chem. **282:**37158–37169.
48. **Shimakami, T., R. E. Lanford, and S. M. Lemon.** 2009. Hepatitis C: recent successes and continuing challenges in the development of improved treatment modalities. Curr. Opin. Pharmacol. **9:**537–544.
49. **Tellinghuisen, T. L., M. J. Evans, T. von Hahn, S. You, and C. M. Rice.** 2007. Studying hepatitis C virus: making the best of a bad virus. J. Virol. **81:**8853–8867.
50. **Tellinghuisen, T. L., and C. M. Rice.** 2002. Interaction between hepatitis C virus proteins and host cell factors. Curr. Opin. Microbiol. **5:**419–427.
51. **Thompson, A. J., and J. G. McHutchison.** 2009. Antiviral resistance and specifically targeted therapy for HCV (STAT-C). J. Viral Hepat. **16:**377–387.
52. **Tscherne, D. M., C. T. Jones, M. J. Evans, B. D. Lindenbach, J. A. McKeating, and C. M. Rice.** 2006. Time- and temperature-dependent activation of hepatitis C virus for low-pH-triggered entry. J. Virol. **80:**1734–1741.
53. **Wakita, T., T. Pietschmann, T. Kato, T. Date, M. Miyamoto, Z. Zhao, K. Murthy, A. Habermann, H. G. Krausslich, M. Mizokami, R. Bartenschlager, and T. J. Liang.** 2005. Production of infectious hepatitis C virus in tissue culture from a cloned viral genome. Nat. Med. **11:**791–796.
54. **Wootton, S. K., and D. Yoo.** 2003. Homo-oligomerization of the porcine reproductive and respiratory syndrome virus nucleocapsid protein and the role of disulfide linkages. J. Virol. **77:**4546–4557.
55. **Zhou, S., and D. N. Standring.** 1992. Cys residues of the hepatitis B virus capsid protein are not essential for the assembly of viral core particles but can influence their stability. J. Virol. **66:**5393–5398.
56. **Zhou, S., and D. N. Standring.** 1992. Hepatitis B virus capsid particles are assembled from core-protein dimer precursors. Proc. Natl. Acad. Sci. U. S. A. **89:**10046–10050.
57. **Zweig, M., C. J. Heilman, Jr., and B. Hampar.** 1979. Identification of disulfide-linked protein complexes in the nucleocapsids of herpes simplex virus type 2. Virology **94:**442–450.

Strain-Dependent Viral Dynamics and Virus-Cell Interactions in a Novel *In Vitro* System Supporting the Life Cycle of Blood-Borne Hepatitis C Virus

Hussein Hassan Aly,[1,2] Yue Qi,[3] Kimie Atsuzawa,[4] Nobuteru Usuda,[4] Yasutsugu Takada,[5] Masashi Mizokami,[6] Kunitada Shimotohno,[7] and Makoto Hijikata[1,3]

We developed an *in vitro* system that can be used for the study of the life cycle of a wide variety of blood-borne hepatitis C viruses (HCV) from various patients using a three-dimensional hollow fiber culture system and an immortalized primary human hepatocyte (HuS-E/2) cell line. Unlike the conventional two-dimensional culture, this system not only enhanced the infectivity of blood-borne HCV but also supported its long-term proliferation and the production of infectious virus particles. Both sucrose gradient fractionation and electron microscopy examination showed that the produced virus-like particles are within a similar fraction and size range to those previously reported. Infection with different HCV strains showed strain-dependent different patterns of HCV proliferation and particle production. Fluctuation of virus proliferation and particle production was found during prolonged culture and was found to be associated with change in the major replicating virus strain. Induction of cellular apoptosis was only found when strains of HCV-2a genotype were used for infection. Interferon-alpha stimulation also varied among different strains of HCV-1b genotypes tested in this study. *Conclusion:* These results suggest that this *in vitro* infection system can reproduce strain-dependent events reflecting viral dynamics and virus-cell interactions at the early phase of blood-borne HCV infection, and that this system can allow the development of new anti-HCV strategies specific to various HCV strains. (HEPATOLOGY 2009;50:689-696.)

Hepatitis C virus (HCV) is a serious problem worldwide, with 3% of the world's population chronically infected.[1] Chronic infection with HCV may lead to high rates of liver cirrhosis and hepatocellular carcinoma.[2] Because the HCV standard therapy is still insufficient for treating many patients,[3] the development of more effective and less toxic anti-HCV agents is desired. The virological studies required to reach this goal need reproducible and efficient HCV proliferation in cell culture. An *in vitro* infection system using recombinant HCV-JFH1 was developed. In this system, HuH7 cells transfected with *in vitro*-synthesized JFH1-RNA were

Abbreviations: 2D, two-dimensional; 2D-HuS-E/2, HuS-E/2 cells cultured in two-dimensional condition; 3D, three-dimensional; 3D/HF, 3D hollow fibers; 3D-HuS-E/2, HuS-E/2 cells cultured in three-dimensional condition in the hollow fibers; HCV, hepatitis C virus; IFN-α, interferon alpha; LDH, lactate dehydrogenase; p.i., postinfection; RFB, radial-flow bioreactor; RT-PCR, reverse transcription polymerase chain reaction.

From the [1]Laboratory of Human Tumor Viruses, Institute for Virus Research, Kyoto University, Kyoto, Japan; [2]Hepatology Department, National Hepatology and Tropical Medicine Research Institute, Cairo, Egypt; [3]Laboratory of Viral Oncology, Graduate School of Biostudies, Kyoto University, Kyoto, Japan; [4]Department of Anatomy, Fujita Health University School of Medicine, Toyoake, Japan; [5]Department of Surgery, Division of Hepato-Pancreato-Biliary and Transplant Surgery, Graduate School of Medicine, Kyoto University, Kyoto, Japan; [6]Research Center for Hepatitis and Immunology, International Medical Center of Japan Kounodai Hospital, Ichikawa, Japan; [7]Center for Human Metabolomic Systems Biology, Keio University, Tokyo, Japan.

Received November 12, 2008; accepted April 9, 2009.

Supported by grants-in-aid from the Ministry of Health, Labor and Welfare of Japan; by grants-in-aid from Japan Health Sciences Foundation; and by grants-in-aid for scientific research from Ministry of Education, Sports, Culture, and Technology of Japan.

Address reprint requests to: Kunitada Shimotohno, Ph.D., Center for Human Metabolomic Systems Biology, Keio University, 35, Shinano-machi, Shinjuku-ku, Tokyo, 160-8582, Japan. E-mail: shimkuni@z8.keio.jp; fax: 81-3-5363-3592; or Makoto Hijikata, Ph.D., Laboratory of Human Tumor Viruses, Institute for Virus Research, Kyoto University, 53, Kawaharacho, Shogoin, Sakyoku, Kyoto, 606-8507, Japan. E-mail: mhijikat@virus.kyoto-u.ac.jp; fax: 81-75-751-3998.

Published online in Wiley InterScience (www.interscience.wiley.com).

DOI 10.1002/hep.23034

Potential conflict of interest: Nothing to report.

Additional Supporting Information may be found in the online version of this article.

shown to secrete infectious viral particles.[4] This system, however, requires the combination of HuH-7-derived cell lines and JFH1-based constructs, limiting its usefulness for studying other HCV strains. Because HuH-7 cells cannot support the complete life cycle of blood-borne HCV (bbHCV) derived from clinical samples,[5] this system is insufficient for studying all the events related to bbHCV infection.

Many researchers have attempted to develop an *in vitro* system for bbHCV.[6-8] These current systems, however, are still insufficient due to their low efficiency for infectivity and replication of bbHCV. Working toward this same goal, we recently established immortalized primary human hepatocyte cell lines by transducing them with E6 and E7 genes from the human papilloma virus 18.[5,9] As expected, we observed improved infection and replication of bbHCV especially in one of these cell lines (HuS-E/2 cells) that showed a similar expression profile to that of human primary hepatocytes, but this strategy did not improve production of infectious particles.

Recently, a hybrid artificial liver support system was developed using animal hepatocytes cultured in a three-dimensional hollow fiber (3D/HF) system. This bioartificial liver showed several characteristic features of liver tissue for more than 4 months.[10-12] By growing our HuS-E/2 cells in a similar 3D culture[5] the gene expression profile was improved to more closely match that of human primary hepatocytes. Because the 3D cell culture condition more closely reproduces the *in vivo* environment of hepatocytes,[13] culturing these cells in this manner may support the entire HCV life cycle.

In this study we utilized this small 3D culture system and showed it to be ideal for culturing HuS-E/2 cells for the study of bbHCV infection. Using this system we are now able to study the variable patterns of the life cycle of different bbHCV strains as well as HCV-related cellular events.

Materials and Methods

Cell Culture. HuS-E/2 cells were cultured as previously described.[5] For the 3D/HF system, HuS-E/2 suspension was injected into the lumen of HF (Toyobo, Osaka, Japan) made from cellulose acetate and containing pores for nutrients and waste exchange (Supporting Fig. 1). The bundles were centrifuged to induce organoid formation. The cells in the fibers were cultured in 12-well plates (two capillary bundles per well) with gentle rotation using serum-free medium (Toyobo) in a CO_2 incubator at 37°C. The number of cells was adjusted to 3×105 cells per two-capillary bundle at the start of each experiment.

RNA Experiments. Total RNA was extracted from two-dimensional (2D) cultured cells, patient sera, or from 100 times concentrated culture medium as previously described.[4,5] For cells cultured in the 3D/HF, sterile scissors were used to cut each fiber into small pieces (1 mm^2 each), which were then solubilized in Sepasol RNA-1 (Nacalai Tesque, Kyoto, Japan). RNA was then extracted according to the manufacturer's protocol. Real-time reverse transcription polymerase chain reaction (RT-PCR) was performed as described.[5]

HCV Infection. HCV infection experiments were carried out using sera from HCV patients. The amount of each inoculum was adjusted so as to add similar amount of HCV-RNA to the medium of the cells. After 24 hours, the cells were washed three times with phosphate-buffered saline (PBS) and cultured for the designated times. To assess the passage of infectivity, 12 mL of culture medium from the primary infected cells was collected, concentrated 100 times by filtration through Amicon Ultra-15, Ultracel-10K filters (Millipore, Carrigtwohill, Cork, Ireland), and 40 μL concentrated medium/well was used to infect naïve HuS-E/2 cells. All experiments were done with approval of the Ethical Committee of Kyoto University. Informed consent from patients was required for this approval.

Cloning and Sequencing. To amplify the complementary DNA (cDNA) fragment corresponding to hypervariable region 1 (HVR-1),[14] a nested RT-PCR was performed using Superscript III (Invitrogen, Carlsbad, CA) and PrimeSTAR HS DNA Polymerase (Takara, Tokyo, Japan). Reaction conditions were adjusted according to the manufacturer's protocol. Primers used were previously described[15] and are shown in Supporting Table 1. PCR products were then purified and cloned using the Zero Blunt TOPO PCR Cloning Kit (Invitrogen). Ten recombinant clones were randomly isolated for each PCR product and sequenced as described.[16]

Quantitative Detection of HCV Core and Interferon alpha (IFN-α) Protein by Enzyme-Linked Immunosorbent Assay (ELISA). The culture medium of infected cells was collected and concentrated 100 times as previously mentioned for the detection of HCV-core, or used directly for detection of IFN-α. HCV core protein was quantified using the Trak-C Core ELISA (Ortho Clinical Diagnostics, Neckargemünd, Germany). IFN-α was quantified using the Human IFN-A ELISA kit (PBL Biomedical Laboratories, Piscataway, NJ). Light absorbance was then measured using a Wallac 1420 multilabel counter (PerkinElmer Life Science, Waltham, MA).

Cytotoxicity Assay. Culture medium was collected from HCV-infected cells and used for measuring lactate dehydrogenase (LDH) levels using an LDH cytotoxicity

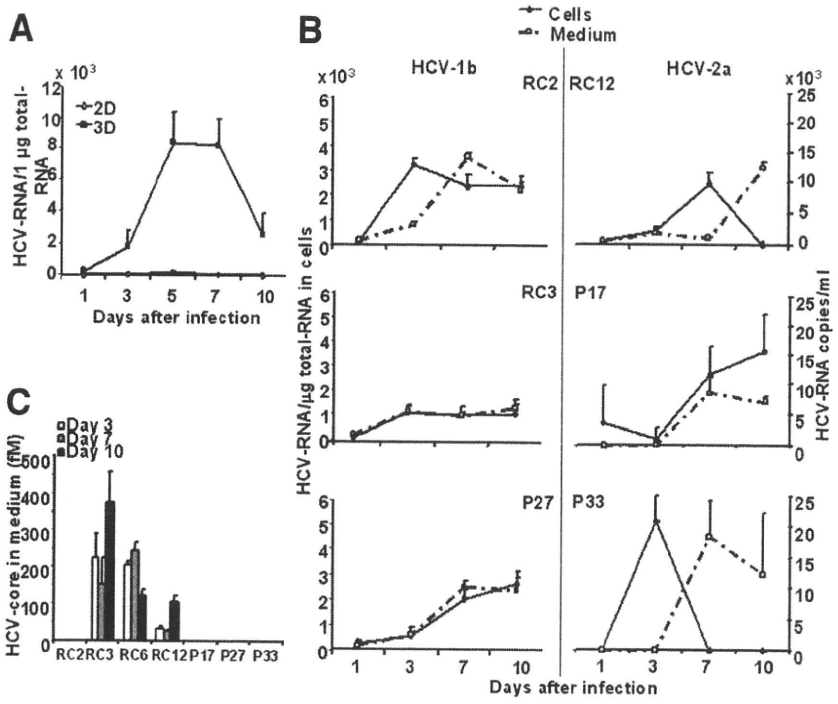

Fig. 1. Infection and proliferation of bbHCV in 3D-HuS-E/2 cells. (A) The quantity of HCV genomic RNA in 1 μg total RNA of 2D- or 3D-HuS-E/2 cells infected with HCV-RC6 was determined at each timepoint after infection by real-time RT-PCR analysis. (B) 3D-HuS-E/2 cells were infected with HCV-1b-containing sera: RC2, RC3, and P27; or HCV-2a-containing sera: 4: RC12, P17, P33. The quantity of HCV genomic RNA in the infected cells was determined as in (A). The culture medium from the last 2 days at each timepoint was collected, concentrated, and the amount of HCV-RNA (B) or HCV-core (C) was measured. Data represent the mean ± standard deviation (SD) of three independent experiments.

detection kit (Takara Biomedicals). Light absorbance was then measured as described above.

Sucrose Density Gradient. The culture medium of the infected cells was collected, concentrated 500 times, and loaded onto a 20%-50% (wt/vol) sucrose gradient containing 50 mM PBS, 100 mM NaCl, and 1 mM EDTA, followed by centrifugation at 100,000*g* for 16 hours at 4°C in a SW41Ti rotor (Beckman, Fullerton, CA). The gradient was fractionated into 31 fractions that were used for HCV-RNA and core detection and HCV infection into naïve cells as described above.

Electron Microscopy. The 1.12 g/mL fraction obtained by the sucrose density gradient showed the secondary infection activity as analyzed by transmission electron microscopy. The fraction was ultracentrifuged and the almost all supernatant was removed. The residual 10 μL of the solution was directly applied to a formvar-carbon grid for negative staining with 1% uranyl acetate solution and observed with an electron microscope (JEOL1010, JEOL, Tokyo, Japan).

Results

HuS-E/2 Cells Cultured in 3D/HF System Are Highly Permissive for Infection and Proliferation of bbHCV. We compared the ability of HuS-E/2 cells cultured in the 3D/HF system (3D-HuS-E/2 cells) to those cultured as a monolayer (2D-HuS/E2 cells) to reproduce infection by HCV genotype 1b (HCV-RC6), derived from patient serum (RC6). The HCV-RC6 RNA levels in the 3D-HuS/E2 cells were significantly higher at all timepoints (Fig. 1A), showing that the 3D/HF system greatly improves the proliferation of bbHCV in HuS-E/2 cells. We observed that both the early stages of infection and the continuous replication of HCV-RC6 in HuS-E/2 cells was improved by 3D/HF culture when the culture conditions were changed after the infection from 3D/HF to 2D and vice versa (Supporting Fig. 2).

As reported,[17] blocking CD81, an HCV-supposed entry receptor, during infection significantly impaired HCV proliferation into 3D-HuS-E/2 cells (Supporting Fig. 3), suggesting that CD81 is essential for HCV infectivity in 3D-HuS-E/2 cells. Although the expression level of CD81 mRNA in 3D-HuS-E/2 cells was observed, no significant change from 2D-HuS/E2 cells was found (data not shown), indicating that the quantity of CD81, at least, is not responsible for the improvement.

We then examined whether this system can be used for proliferation of six different bbHCV samples, three of which are HCV-1b (HCV-RC2, HCV-RC3, and HCV-P27) and three HCV-2a genotypes (HCV-RC12, HCV-P17, and HCV-P33) (Fig. 1B). Proliferation of HCV-RNA in the cells was seen in all six cases, suggesting that this system can be widely used for analysis of infection and proliferation of bbHCV strains. HCV-RNA and HCV-core were also detected in the culture medium (Fig. 1B). Different HCV strains showed variable patterns of proliferation and HCV-core secretion into the medium. Although HCV-core was detected from day 3 onward when

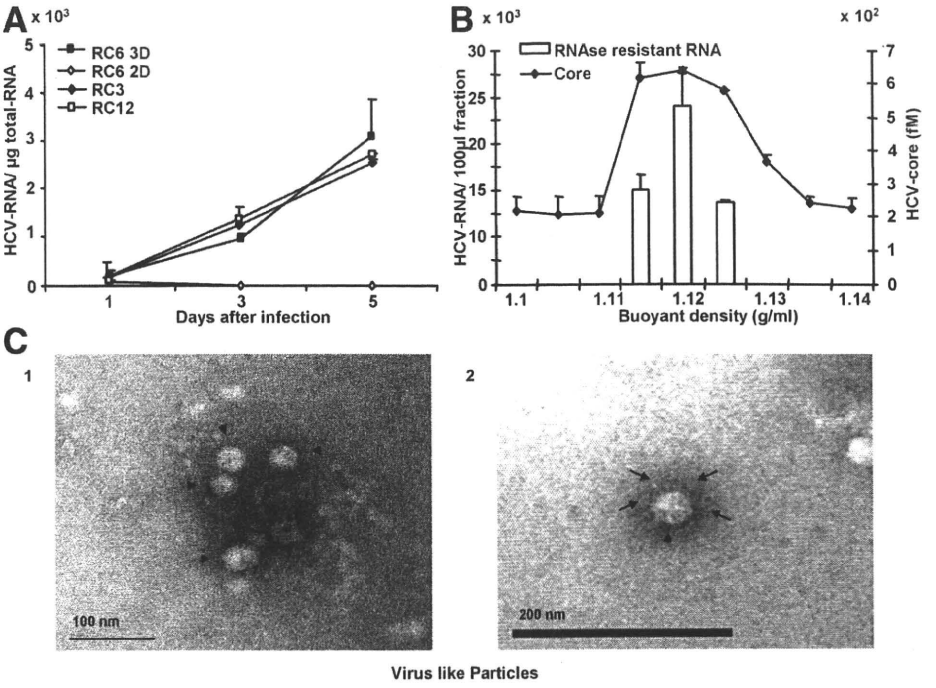

Fig. 2. Production of infectious virus-like particles from 3D-HuS-E/2 cells infected with different HCV strains. (A) The culture medium of 3D-HuS-E/2 cells infected with HCV-RC3 or HCV-RC6 was collected from days 5 to 7 p.i. and for HCV-RC12 from days 23 to 25 p.i. The culture medium of 2D-HuS-E/2 cells infected with HCV-RC6 was also collected from days 5 to 7 p.i., and used to treat naïve 3D-HuS-E/2 cells. The quantity of HCV genomic RNA in 1 μg of total cellular RNA was determined as in Fig. 1. (B) The concentrated culture medium of 3D-HuS-E/2 cells infected with HCV-RC3 was collected from days 5 to 7 p.i., and fractionated by ultracentrifugation with a 20%-50% sucrose density gradient. HCV-core protein and the RNase A-resistant HCV-RNA in the different fractions were quantitatively analyzed using an HCV-core ELISA kit and real-time RT-PCR, respectively. Data represent the mean ± SD of three independent experiments. (C) Photomicrograph showing negatively stained virus-like particles from the culture medium of HCV-RC3-infected 3D-HuS-E/2 cells (arrowheads, panels 1 and 2). The arrows indicate the spike-like structures found on the surface of the virus-like particles (panel 2).

RC3, RC6, and RC12 were used for infection, it was undetectable when RC2, P17, P27, and P33 sera were used, similar to 2D-HuS-E/2 cells infected with HCV-RC6 (Fig. 1C).

Production of Infectious Particles from 3D-HuS-E/2 Cells Infected with bbHCV. The culture media from 2D or 3D-HuS/E2 cells infected with RC6 serum (Fig. 1A) were collected from days 5 to 7 postinfection (p.i.), concentrated, and inoculated into naïve 3D-HuS-E/2 cell culture media. HCV-RNA's proliferation in the infected cells was only detected when using the culture medium from 3D-HuS-E/2 cells and not 2D-HuS-E/2 cells (Fig. 2A). Media collected from HCV-RC3 at days 5 to 7 and from HCV-RC12 from days 23 to 25 p.i. were also able to infect naïve cells (Fig. 2A). These data suggested the production and secretion of infectious virus-like particles. To investigate this further, biophysical analysis was performed. The culture medium of HCV-RC3 infected 3D-HuS-E/2 cells at day 7 p.i. was fractionated using a sucrose density gradient after RNase A treatment. HCV core was detected in the 1.11 to 1.14 g/mL fractions; similarly, the nuclease-resistant HCV RNA peaked in the 1.12 g/mL fraction (Fig. 2B). Furthermore, only the 1.12 g/mL fraction was able to infect naïve cells as examined above (data not shown). This fraction was pelleted by ultracentrifugation and examined by electron microscopy with negative staining. We observed 33-nm to 45-nm diameter spherical particles (Fig. 2C, panel 1) with spike-like structures from 7-9 nm in length on the surface (Fig. 2C, panel 2), consistent with HCV morphology reported previously in HCV patients.[18] These were detected in the sample collected from HCV-RC3-treated but not mock-treated 3D-HuS-E/2 cells. These data suggest that production of infectious virus-like particles occurs in 3D-HuS-E/2 cells infected with some bbHCV strains. It is therefore likely that 3D-HuS-E/2 cells can be used to reproduce nearly all steps in the HCV life cycle.

Prolonged Culture of HCV-Infected Cells in the 3D Hollow Fiber System. For HCV-RC6-infected cells (Fig. 3A), the amount of HCV-RNA in the cells fluctuated during the 30-day culture period. The levels of both HCV-RNA and HCV-core in the medium showed a similar pattern of fluctuations that peaked on days 5 and 20 p.i. Unlike RC6, the pattern of HCV-RNA levels in the medium of RC12-infected cells showed a negative

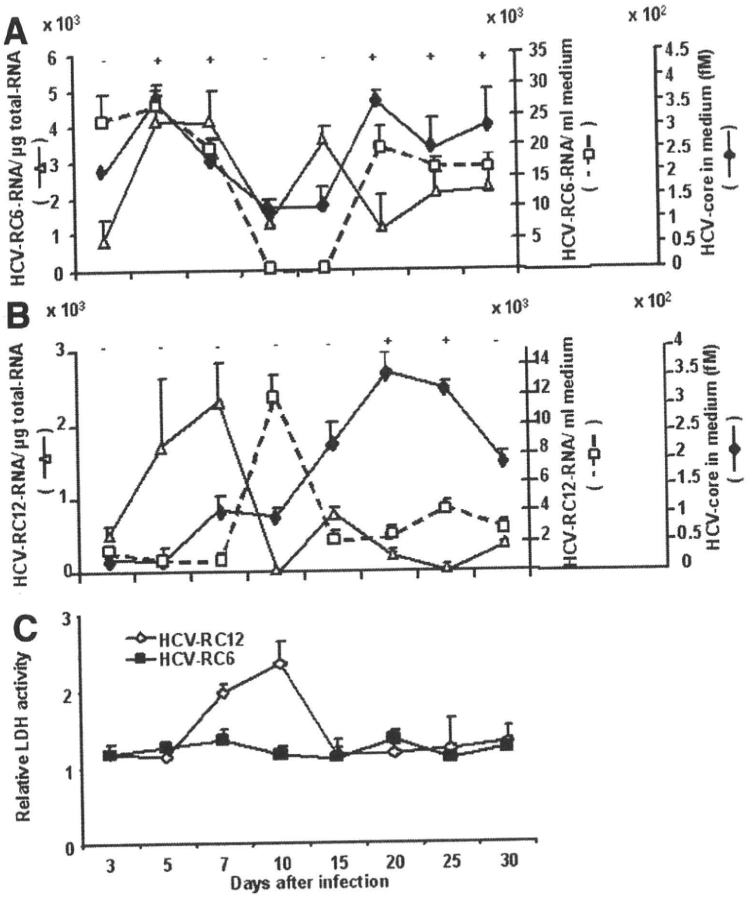

Fig. 3. Prolonged culture of HCV-infected cells in the 3D/HF system. After infection with HCV-RC6 (A) and HCV-RC12 (B), 3D-HuS-E/2 cells were cultured for 30 days with a medium change every 2 days. The HCV-RNA in the cells and medium as well as the HCV-core in the medium were quantitatively analyzed at the designated timepoints as in Fig. 1. Culture media were also used to treat naïve 3D-HuS-E/2 cells to examine the secondary infection as in Fig. 2. (+) and (−) indicate detection or no detection of secondary infection. (C) Culture media of HCV-RC6 and HCV-RC12 infected cells collected at each timepoint were used for the detection of LDH levels released from dead cells. LDH levels were normalized to uninfected cells cultured for the same time. Data represent the mean ± SD of three independent experiments.

correlation with that detected in the cells. This was clearly seen on day 10 p.i., when a sharp increase and decrease of HCV-RNA in the medium and the cells, respectively, was observed (Fig. 3B). Similarly, the amount of HCV-core detected in the medium throughout the culture was not correlated with RNA levels in the medium. Instead, core levels were very low in the first 10 days, at which time levels increased, reaching a peak on day 20 p.i. (Fig. 3B). Culture media from cells infected with HCV-RC6 from days 5 to 7 and 20 to 30 p.i. (Fig. 3A) and that from HCV-RC12 from days 20 to 25 p.i. showed passage of infectivity (Fig. 3B). All culture media showing infectivity appeared to have a high amount of HCV-core protein.

Clonal Changes in HCV During Prolonged Culture. In order to perform a populational analysis to understand the fluctuating pattern seen during HCV proliferation, two sera with limited HCV variants, HCV-RC6 (two major strains) and -RC12 (single major strain) from immunosuppressed liver transplantation patients with recurrent HCV were used in the previous prolonged infection experiment. The variants' composition was analyzed by single-strand confirmation polymorphism analysis for HCV-HVR1 (Supporting Fig. 4). RC6 serum (Fig. 4A) showed two different major sequences, HCV-RC6-1 and -2 strains, which constituted 60% and 40%, respectively, and shared 85% homology. In cells infected with HCV-RC6 the nucleotide sequence of HVR1 on day 5 showed 97% homology to HCV-RC6-1, and on day 20 p.i. it showed 97% homology to HCV-RC6-2. These data suggest selection of the dominant HCV strain in the cells over time. For RC12 (Fig. 4B), the nucleotide sequence on day 5 p.i. had only one nucleotide difference from that of the HCV from the original serum. The sequence from day 20 p.i. was four nucleotides different from that from the serum, and five different from the cells on day 5 p.i. These data indicated that each peak of HCV-RNA that appeared in the cells infected with RC12 serum included primarily a single HCV strain with a slightly different genomic sequence. This suggests that the periodic appearance of HCV-RNA peaks in the cells infected with a particular HCV strain is a result of selection and/or mutation of HCV strains during the prolonged culture period.

Cellular Response Induced by bbHCV Infection. At day 10 p.i., HCV-RNA levels in the culture medium rose and RNA levels in 3D-HuS-E/2 cells infected with HCV-RC12 dropped (Figs. 1B, 3B). To determine if this was caused by a cytotoxic effect of HCV infection, LDH levels were measured in the culture medium of HCV-RC6- and

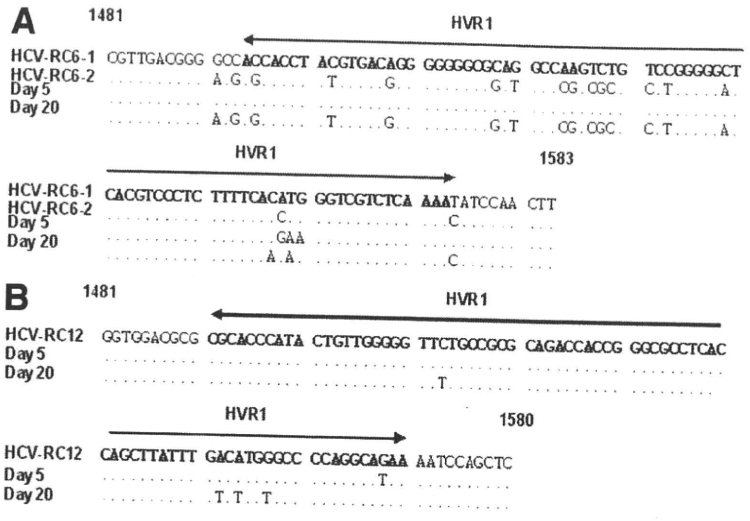

Fig. 4. Comparison of HCV-HVR1 sequences in the serum used for infection and the HCV replicating in the cells on days 5 and 20 after infection of HCV-RC6 (A) or HCV-RC12 (B). Nucleotide numbering was based on HCV-J1 sequence (GenBank Access. No. D10749). Three additional nucleotides were found at the 5′-terminal end of the E2 regions of all RC6 sequences. The major sequence present in the serum used for infection is shown in the upper row in each panel. Dots represent the identical nucleotides.

HCV-RC12-infected 3D-HuS-E/2 cells. LDH activity showed a strong correlation with HCV-RNA levels in the medium on day 10 p.i. in HCV-R12-infected cells (Fig. 3B), suggesting a cytotoxic effect of HCV-RC12 that was not observed in the case of HCV-RC6 (Fig. 3A,C). To determine if this HCV infection-mediated cytotoxicity is due to apoptosis, as with other viruses belonging to the Flaviviridae family,[19] the involvement of caspase was examined using the caspase inhibitor z-VAD-fmk. A significant dose-dependent reduction in HCV-RNA levels in the medium and LDH activity (Fig. 5A,B) was found, whereas no significant effect was observed on the viability of noninfected cells (Fig. 5B) or intracellular HCV-RNA levels (Fig. 5A). This suggested that the cytotoxic effect of HCV infection is mediated by apoptosis. It is noteworthy that HCV-induced cytopathicity was also found when HCV-P17 and HCV-P33 samples were used for infection (both are HCV-2a genotype) and was not reproduced in any of the HCV-1b genotype samples used in this work (Fig. 5C).

After infection with HCV-RC6, no cytotoxicity was detected that might have inhibited HCV-RC6-1 proliferation in the cells. However, HCV-RC6-2 RNA replaced HCV-RC6-1 RNA during prolonged culture. To assess a

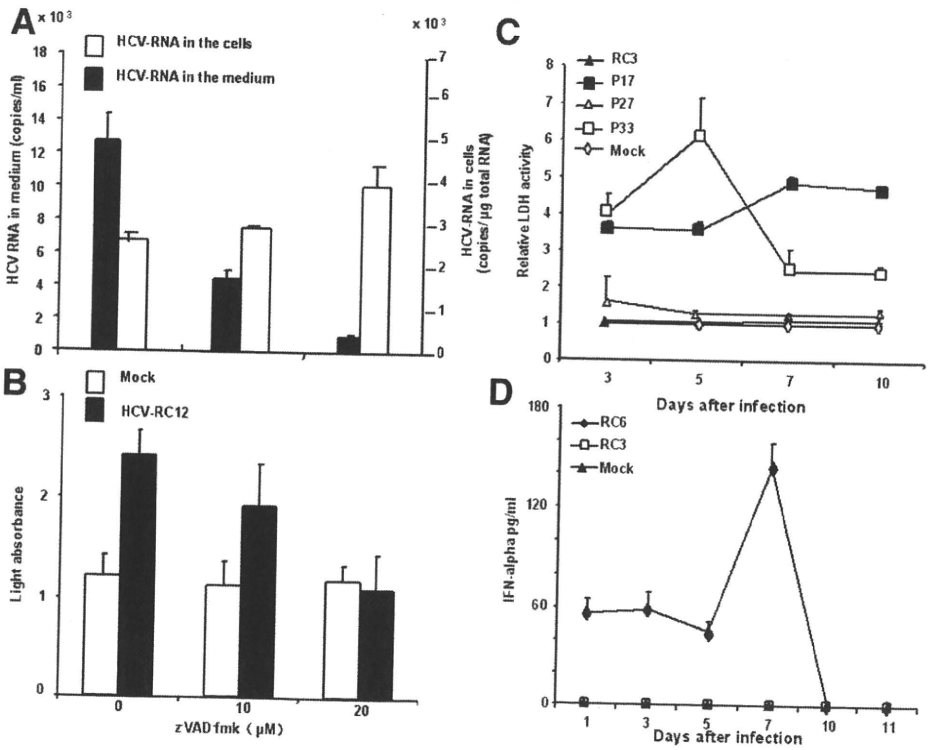

Fig. 5. Cellular response of 3D-HuS-E/2 cells infected with bbHCV. 3D-HuS-E/2 cells infected with HCV-RC12 and mock-treated cells were cultured for 10 days in the presence of z-VAD-fmk (0, 10, and 20 μM). (A) HCV-RNA in the cells and medium on day 10 was measured as in Fig. 1. (B) LDH levels in the medium on day 10 after infection with HCV-RC12 was measured as in Fig. 3. (C) Culture media of HCV-RC3, HCV-P17, HCV-P27, HCV-P33, and mock-infected cells collected at designated points were used for the detection of LDH levels. (D) IFN-α levels in the culture media of HCV-RC6, HCV-RC3, and mock-infected cells collected at each designated timepoint were measured by ELISA. Data represent the mean ± SD of three independent experiments.